Journal of Materials Chemistry C

ROYAL SOCIETY OF CHEMISTRY

REVIEW

View Article Online
View Journal | View Issue

Check for updates

Cite this: *J. Mater. Chem. C*, 2024, **12**, 1923

# Symphony of light: AIE and MFC in carbazole-based cyanostilbenes

A. Afrin and P. Chinna Ayya Swamy *

In the realm of molecular design, carbazole-based cyanostilbenes have emerged as captivating conjugates, attracting researchers with their unique characteristics such as aggregation-induced emission (AIE) and mechanofluorochromism (MFC). This comprehensive review explores their distinct features, especially AIE and MFC, and provides illumination of the assumptions underlying these conjugates, their intricate structural modifications, and their potential applications. The introductory section provides a foundation for understanding solid-state emissive properties, *i.e.*, AIE and MFC, elucidating the fundamental mechanisms driving these phenomena. Additionally, we have carefully categorised and classified various carbazole-based cyanostilbene molecules that display AIE and MFC characteristics, providing readers with a methodical summary of the variety within this fascinating family of conjugates. A substantial portion is dedicated to an in-depth analysis of the most notable examples of carbazole-based cyanostilbenes displaying AIE and MFC, emphasizing their molecular structures, and the impact of external stimuli on their optical properties in solution as well as the solid state. The most recent advances in the area are discussed, along with an in-depth investigation of the mechanisms governing AIE and MFC in these compounds, taking into account the significance of structural changes and intermolecular interactions. Additionally, this review explores the prospective uses of carbazole-based cyanostilbenes, exploring their potential in fields including bioimaging, sensors, optoelectronics and organic light-emitting diodes (OLEDs). The future outlook in these areas is discussed, offering valuable insights into the promising avenues of research and development in the years to come.

Received 10th November 2023,
Accepted 2nd January 2024

DOI: 10.1039/d3tc04121b

rsc.li/materials-c

Open Access Article. Published on 04 January 2024. Downloaded on 7/20/2025 3:37:24 PM.
This article is licensed under a Creative Commons Attribution-NonCommercial 3.0 Unported Licence.

*Main group Organometallics Optoelectronic Materials and Catalysis Lab, Department of Chemistry, National Institute of Technology, Calicut, 673601, India. E-mail: swamy@nitc.ac.in*

**A. Afrin**

*Afrin A Afrin A completed her Master's degree in Chemistry at Cochin University of Science and Technology in the year 2020. She started her research career as a Project Associate in Dr Swamy's lab in the year 2022, and later joined as a PhD student in July 2023. Her research areas is focused on modulation of solid-state emissive properties of donor–acceptor conjugates.*

**P. Chinna Ayya Swamy**

*Chinna Ayya Swamy P Dr Swamy obtained his MSc in General Chemistry from the University of Hyderabad in 2009 and his PhD from the IISc, India, in the field of main-group organometallics in 2014. After completion of his PhD, he spent five years abroad as a post-doctoral fellow in the area of supramolecular chemistry and organometallic chemistry. Later, he joined the Department of Chemistry, National Institute of Technology, Calicut, as an Assistant Professor in 2020. Currently, he works on the design and synthesis of supramolecular architectures for stabilizing low-valent main-group compounds, metal-based asymmetric catalysis and chemosensors for biologically important ions.*

Open Access Article. Published on 04 January 2024. Downloaded on 7/20/2025 3:37:24 PM. This article is licensed under a Creative Commons Attribution-NonCommercial 3.0 Unported Licence.

# 1. Introduction

Solid-state emissive organic fluorophores are a class of compounds with remarkable optical properties and represent potential candidates in various fields, including biology,[1–5] materials science,[6–9] and optoelectronics.[10–16] In general, organic fluorophores possess weak emission in the solid state due to the presence of π–π stacking, which leads to self-absorption of the molecules and causes non-radiative pathways to be followed. The introduction of bulky substituents on organic fluorophores prevents the π–π stacking, resulting in strong luminescence in the solid state. On the other hand, molecules tend to form aggregates, and the restriction of free rotation leads to enhanced emission. Furthermore, this unique property stems from the intricate electronic structure of organic fluorophores, which show a strong fluorescent nature as compared to inorganic metal complexes. Solid-state emissive organic fluorophores, have many potential applications and are extensively employed as vital tools in organic light-emitting diodes (OLEDs), molecular lasers, security and cellular imaging.[17,18] In the last decade, researchers have focused on the synthesis of organic fluorophores that emit in the solid and aggregated states, which have been found to have potential in biology, such as to visualize and track cellular processes, study protein interactions, and illuminate intricate molecular mechanisms.

Further, the realm of optoelectronics has seen substantial advances through the integration of organic fluorophores, which display very good emission in the solid state, and such materials have been found to be potential candidates for organic light-emitting diodes (OLEDs)[19–21] and display technologies, as well as in organic photovoltaics (OPVs).[22,23] Nevertheless, creating effective organic fluorophores requires an intricate compromise between their chemical structure and photophysical characteristics, which makes the process difficult.[24–26] In the last decade, researchers have focused on the design and synthesis of novel organic fluorophores with enhanced luminescence, high photostability, and environmental resilience to broaden their scope of application. As the journey of understanding and manipulating light–matter interactions progresses, organic fluorophores have proved to be versatile emissive entities that bridge the gap between fundamental scientific exploration and real-world technological advancements. In this regard, there are several organic fluorophores, such as triphenylamine, tetraphenylethene, anthracene, naphthalenediimide, diketopyrrolopyrrole, BODIPY, diphenyldibenzofulvene and fluorene, that are utilised for OLEDs and display technology. However, the reported organic fluorophores exhibit several disadvantages, such as poor stability, less proximity of color tunability and less efficiency. For organic fluorophores to overcome these drawbacks, find applications in both research and industry and solidify their place as essential luminous agents in the ever-expanding realm of optics and electronics, researchers must understand their potential in design and principle.

The emergence of aggregation-induced emission (AIE) has sparked a revolution in understanding the light–matter interactions shown by organic fluorophores. The concept of AIE developed by Tang *et al.*, in 2001[30] has gained significant attention due to its relevance in various fields, such as materials science, optoelectronics, and bioimaging. AIE represents an intriguing phenomenon in the realm of luminescent materials, wherein certain molecules that are usually non-luminescent in the solution state due to the presence of several non-radiative pathways become extremely fluorescent upon particular aggregation.[27–29] On the other hand, aggregation-caused quenching (ACQ), which is the opposite phenomenon to AIE, is the more commonly observed one. Due to this phenomenon, many organic luminophores display very poor emission in the aggregated state, which might be due to their self-quenching and π–π stacking ability. AIE-active materials exhibit bright luminescence due to the restriction of inter-molecular motion and conformational changes, as the molecules are packed closely together in aggregates. AIEgens have been developed as a new class of materials for practical uses, and have found applications in numerous fields including biological labelling, organic light-emitting diodes (OLEDs), imaging agents, molecular sensors, and security.[31–34] Recently, several researchers have focused on the design and synthesis of novel organic fluorophores that emit light more efficiently in the aggregated states, enabling the creation of brighter and more stable luminescent materials. The study of AIE not only provides novel approaches to persistent problems in a variety of technical domains (especially in display technologies), but also enhances the understanding of light–matter interactions and demonstrates the inventiveness of researchers in using unusual behaviours for useful applications.

Another interesting phenomenon is mechanofluorochromism (MFC),[35–38] which is the alteration of a material's fluorescence characteristics in response to mechanical stimuli such as grinding, shearing, or pressure, which gives rise to another fascinating class of organic fluorophores. In other words, the emission of light from the material changes when it undergoes mechanical deformation. MFC materials are a subset of the broader field, which involves changes in solid-state emission or the color of fluorescence due to mechanical forces, and have been mainly applied in sensors, smart materials, security inks, and other innovative technologies.[39,40] There are no precise processes driving MFC; the phenomenon depends on the orientation of the organic fluorophores, and the molecular configuration, electrical structure, and energy transfer routes of the materials are frequently altered when they are subjected to mechanical stress. Furthermore, the molecular structure, chemical content, and intermolecular interactions of a material all affect its MFC ability. Many researchers have been actively investigating various forms of organic fluorophores that show significant MFC properties recently, including small molecules, polymers, and nanomaterials. The goal is to produce materials with practical uses and obtain a deeper understanding of the underlying processes. MFC offers the potential for real-time visual detection of mechanical stress, which can be valuable in fields such as materials science, engineering, and structural monitoring. Furthermore, these materials may be used to develop self-reporting systems in which mechanical deformation causes a fluorescence shift that serves as an obvious indicator of

 This journal is © The Royal Society of Chemistry 2024

Open Access Article. Published on 04 January 2024. Downloaded on 7/20/2025 3:37:24 PM.
This article is licensed under a Creative Commons Attribution-NonCommercial 3.0 Unported Licence.

pressure or stress. In this regard, the development of novel MFC materials could lead to advances in a range of technologies and contribute to the development of responsive and adaptable materials that can sense and signal mechanical changes.

Against the ever-evolving landscape of materials science, certain compounds have emerged as captivating focal points, drawing the attention of researchers and innovators alike. In this regarding, we have recently concentrated on the design and synthesis of a number of donor–acceptor conjugates based on carbazole/fluorene and cyanostilbene, which were shown to be suitable candidates for AIE- and MFC-active materials.[41,42] In this review, we delve into the captivating realm of carbazole-based cyanostilbenes, a class of compounds that has garnered significant interest due to its unique attributes. Specifically, we shine a spotlight on two distinct yet interconnected characteristics: aggregation-induced emission (AIE) and mechanofluorochromism (MFC). These properties have ignited a new wave of exploration and potential applications in various fields, ranging from optoelectronics to sensing and beyond. As we journey through the intricate intricacies of these compounds, we unravel their underlying mechanisms, delve into their synthesis techniques, and explore the myriad ways in which they exhibit AIE and MFC phenomena.

## 2. Aggregation-induced emission: illuminating the bright side of molecular assembly

AIE, a phenomenon that is contrary to the conventional one, challenges the notion that molecular aggregation inevitably results in luminescence quenching. Instead, it demonstrates a remarkable finding: certain molecules that are typically non-emissive when dispersed in solution become emissive as they aggregate in a solid or condensed state.[30] This transformation challenges traditional quenching effects and has revolutionized the design of luminophores that show strong luminescence in the aggregated state for applications across disciplines.[31–34] Upon molecular aggregation, the inhibition of restricted intramolecular motions takes place, which leads to the emergence of bright emission that is finely tuned by the degree of aggregation. Molecules exhibiting AIE are strategically designed with structures that restrict intramolecular motion, a phenomenon known as the restriction of intramolecular motions (RIM). This restriction prevents non-radiative pathways, favouring radiative decay and resulting in enhanced fluorescence when molecules aggregate. Strategies such as introducing bulky substituents, incorporating rigid molecular frameworks, and employing covalent bonding all contribute to limiting molecular flexibility, thereby promoting AIE behaviour. Further, conjugation effects also influence AIE, with varying degrees of molecular conjugation allowing for precise tuning of luminescence properties. Through implementation of these development factors, researchers have focused on the creation of materials with AIE properties. As research progresses, the understanding of AIE holds promise for the design and development of novel luminescent materials, ushering in a new era of possibilities across the scientific and technological domains.

## 3. Mechanofluorochromism (MFC): unveiling luminescence through mechanical forces

Mechanochromism has emerged as another captivating phenomenon, in which changes in mechanical stimuli induce alterations in the optical properties of materials. MFC challenges the conventional notion that the luminescence behaviour of a molecule remains constant regardless of its environment. Instead, when mechanical forces are applied, be it through grinding, stretching, or shearing, certain molecules respond by altering their luminescence. This responsive behaviour adds a dynamic dimension to materials, making them ideal candidates for a spectrum of applications.[39,40] The prevailing explanation for mechanofluorochromism (MFC) in aggregation-induced emission (AIE) luminogens revolves around a transformative process between crystalline and amorphous phases. This transition is accompanied by changes in molecular packing and/or molecular conformation within the solid state. While a universal mechanism for this novel phenomenon remains elusive, several key factors, such as crystallinity, crystallization velocity, conformation planarization, and intermolecular interactions have emerged as critical contributors to the MFC process.[38] Crystallinity stands out as a pivotal factor influencing MFC in AIE luminogens. The transition between crystalline and amorphous phases during mechanical stress induces changes in the optical properties. The velocity of crystallization plays a noteworthy role, impacting the kinetics of the phase transition and influencing the extent of mechanofluorochromism observed. Conformation planarization is another significant aspect affecting MFC. Mechanical forces can induce alterations in molecular conformations, leading to planarization of certain molecular moieties. This conformational adjustment further influences the electronic transitions responsible for fluorescence, contributing to the observed responses.

Additionally, intermolecular interactions within a material play a crucial role in the MFC process. Forces applied during mechanical stress may disrupt or enhance these interactions, affecting the overall molecular arrangement and, consequently, the luminescence properties of the material. Despite the absence of universally agreed facts regarding the mechanism, the interplay of these factors provides insights into the complex dynamics behind MFC in AIE luminogens. This comprehensive perspective is essential for advancing the design and application of AIE luminogens with tailored mechanofluorescence behaviors. While several reviews have extensively explored aggregation-induced emission (AIE) and mechanofluorochromism (MFC) across diverse fluorophores,[43] we have narrowed our current focus to the unique domain of carbazole–cyanostilbenes. In the following section, we delve into an in-depth exploration of carbazole and cyanostilbenes, unravelling the brilliance of AIE and MFC within this specific molecular

Open Access Article. Published on 04 January 2024. Downloaded on 7/20/2025 3:37:24 PM. This article is licensed under a Creative Commons Attribution-NonCommercial 3.0 Unported Licence.

framework. Our journey will be illuminated by insights into the literature dedicated to understanding the exceptional luminescent characteristics of carbazole-based cyanostilbenes.

## 4. Carbazole

Carbazole (Fig. 1), which is an organic fluorophore that consists of a fused aromatic structure and has diverse properties, has emerged as a cornerstone of aromatic chemistry that has ignited scientific curiosity for decades.[44] This exploration embarks on a journey through the multifaceted world of carbazole, exploring its structural significance, synthetic versatility, and the numerous applications that illuminate its continuing allure. At the heart of carbazole's charm lies its distinctive tricyclic structure, where two benzene rings unite in harmony with a five-membered nitrogen-containing ring. This arrangement not only imparts a unique resonance profile, but also confers intriguing electronic and photophysical properties. In the last few decades, researchers have utilised the carbazole unit in applications ranging from natural products to its modern role as a building block of organic fluorophores in materials science, illustrating how carbazole's versatility has fascinated chemists across generations. The synthesis of carbazole derivatives through diverse routes including oxidative coupling and C–H functionalization exposes a palette of possibilities for fine-tuning properties and tailoring functionalities.[45,46] This diverse synthetic versatility extends its reach into applications spanning from organic electronics to medicinal chemistry.[47–49] Further, the potential abilities of carbazole in terms of its exceptional electronic properties, charge transport capabilities, and energy transfer characteristics make it an essential component in the development of OLED materials.[50,51] Additionally, due to its donor ability, carbazole can act as a hole transport material,[52,53] host material,[54,55] and exciton manager contribute to the advancement of energy-efficient, vibrant, and long-lasting OLED displays and lighting technologies.[56–58] In addition to its contributions to materials science, carbazole's biological activities have also intrigued researchers. Natural carbazole alkaloids exhibit a range of pharmacological properties, propelling studies into their potential as therapeutic agents against various ailments.[59–61]

## 5. Cyanostilbenes

As progress towards enhanced luminescence continues, the world of organic compounds is continuously revealing new wonders in the effort to harness the fascinating properties of light. Among the organic fluorophores, cyanostilbenes have emerged as notable luminophores, catching the attention of researchers across various disciplines.[62,63] This exploration investigates the world of cyanostilbenes, shedding light on their unique attributes, and applications, as well as the underlying principles that make them shine. Cyanostilbenes, which are characterized by their distinctive molecular structure, exhibit a remarkable interplay between conjugation and electron-withdrawing cyano groups. This combination not only imparts these compounds with distinctive photophysical properties, but also endows them with a versatile nature. Their intriguing fluorescence behavior has paved the way for applications in fields as diverse as organic electronics, photonics, and sensing technologies.[62,63] The ability of cyanostilbenes to produce aggregation-induced emission (AIE) is at the heart of their attractiveness. This unique behavior has revolutionized the design of luminophores for solid-state devices and bioimaging and offers enhanced brightness in the solid state, which could be utilised in OLED fabrication.[64–68] Furthermore, the mechanochromic aspect of cyanostilbenes introduces a responsive dimension, in which mechanical forces trigger changes in emission color. This mechanofluorochromism has found applications in stress sensing, structural health monitoring, and beyond. This class of compounds with diverse applications including optoelectronics and materials science can be synthesized through various methods, such as the Knoevenagel condensation reaction, which involves combining a stilbene precursor with a cyano-group-containing reagent. In summary, the synthetic scheme for cyanostilbene starts with the preparation of a stilbene precursor, which is the aromatic aldehyde or ketone, as the starting material. This undergoes a condensation reaction with an appropriate α,β-unsaturated compound (such as acetophenone) to form the stilbene framework, which is catalysed by a base, such as sodium hydroxide, to facilitate the condensation. Depending on the specific substitution patterns and functional groups desired, variations of the Knoevenagel condensation or other synthetic methods may be employed.[69] Different cyano-containing reagents can be used to introduce the cyano group, allowing for fine-tuning of the optical properties in solution as well as the solid state. In this regard, several researchers have focused on the introduction of various substituents on cyanostilbenes for fine-tuning their optical and electronic properties to serve as versatile building blocks in a range of applications. The synthetic strategies involve the strategic combination of aromatic compounds and cyano-containing reagents through condensation reactions. By manipulating the reaction conditions and precursor molecules, researchers can tailor the properties of cyanostilbenes to suit specific applications in fields like optoelectronics, sensing, and materials science.[64–68]

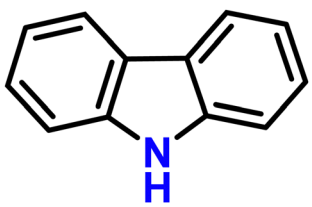


Fig. 1 Structure of carbazole.

## 6. Exploring the brilliance of carbazole-based cyanostilbenes: unveiling AIE and MFC properties

In the field of materials science, the fusion of creativity and innovation often gives rise to compounds that exhibit

 This journal is © The Royal Society of Chemistry 2024

Open Access Article. Published on 04 January 2024. Downloaded on 7/20/2025 3:37:24 PM.
This article is licensed under a Creative Commons Attribution-NonCommercial 3.0 Unported Licence.

exceptional optical properties, which have been examined by various researchers and industries for numerous desirable applications. In this regard, donor–acceptor conjugates based on carbazole and cyanostilbenes represent a prime example of such compounds, attracting attention due to their extraordinary attributes. Carbazole, a versatile aromatic unit, serves as an electron-donating unit, which leads to the observation of interesting optical properties upon its integration with an acceptor. For example, the incorporation of cyanostilbene moieties adds an extra layer of complexity, leading to a synergistic effect that results in remarkable behaviour. This review explores the remarkable world of these compounds, shedding light on two key features that set them apart: aggregation-induced emission (AIE) and mechanofluorochromism (MFC). The AIE phenomenon, wherein molecules become more luminescent upon aggregation, has sparked immense interest because of its potential to enhance light-emitting materials and sensors. Additionally, mechanofluorochromism, which involves changes in emission colour under mechanical stimuli, offers a pathway for dynamic applications in stress-sensing, security and printing. Through a meticulous exploration of synthesis techniques, structural variations, and underlying mechanisms, researchers have begun to unlock the vast potential of carbazole-based cyanostilbenes. Their ability to exhibit pronounced AIE and MFC properties opens doors to an array of applications, ranging from OLED technology and bioimaging to advanced encryption methods. As we journey deeper into the realm of these compounds, we discover a world of untapped possibilities, where the brilliance of light and mechanical force converges to create a new dimension of materials with unparalleled functionalities.

## 7. Carbazole–cyanostilbene based highly fluorescent microcrystals

In 2011, the Neckers group designed the first novel carbazole-based cyano-stilbene derivative (**1**) (Fig. 2), which exhibits aggregation-induced emission enhancement (AIEE).[70] Compound (**1**) can assemble into microcrystals and causes a blue-shift with an enhancement of the intensity of emission in the aggregated state. The nonradiative decay channel restriction of the intramolecular charge transfer (ICT) or twisted intramolecular charge transfer (TICT) states of compound **1** was found to be a primary cause of the AIEE phenomenon (Fig. 2). This emission amplification in the aggregated state is caused by weak molecular stacking in the crystal lattice, which is prevented by intermolecular H-bonding contacts between the discrete dimers of compound **1** and may impede exciton transport through the molecular assembly. The peculiar blue-shift in the emission maximum seems to be caused by conformational twisting in the crystal packing under the aggregated conditions. Furthermore, the fluorescence quenching properties of compound **1** microcrystals enable its use as a highly selective chemosensor for the detection of Cr(VI) in aqueous solution.

## 8. Indolo-carbazole cyanostilbene derivatives

Indolocarbazole cyanostilbenes are a specific class of organic fluorophores that combine the structural features of both indolocarbazoles and cyanostilbenes. Indolocarbazoles are a

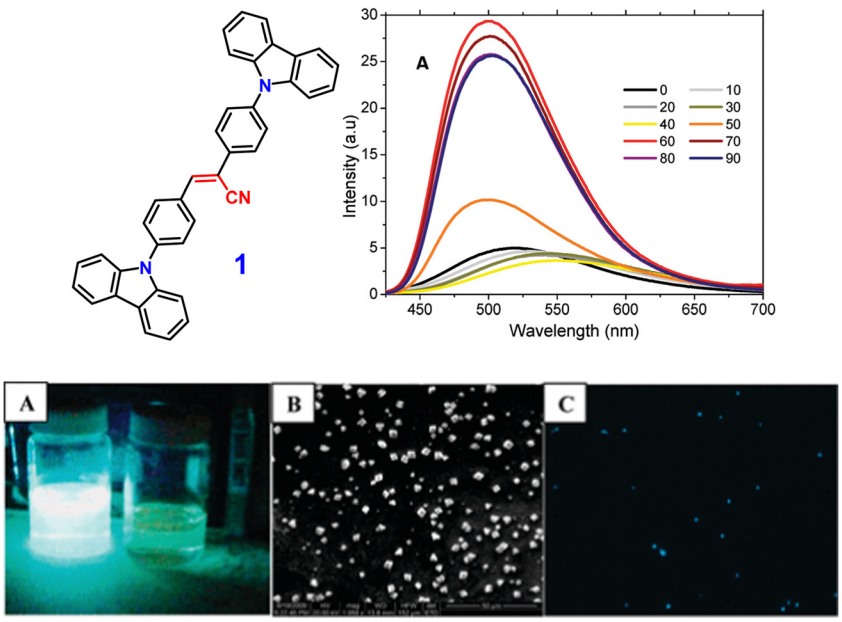


Fig. 2 Above: Structure of compound **1** (left), emission spectra of compound **1** in acetone–water mixtures; concentration = 10 μM, $\lambda_{exc}$ = 360 nm (right). Below: (A) image of compound 1 taken in an acetone–water (40 : 60 v/v) mixture (left) and in pure acetone (right) under 365 nm UV light. (B) SEM image of compound **1** in an acetone–water (40 : 60 v/v) mixture. (C) Fluorescence microscopy image of microcrystals of compound **1** in an acetone–water (40 : 60 v/v) mixture. Reproduced with permission from ref. 70. Copyright 2011 the American Chemical Society.

Open Access Article. Published on 04 January 2024. Downloaded on 7/20/2025 3:37:24 PM.
This article is licensed under a Creative Commons Attribution-NonCommercial 3.0 Unported Licence.

family of molecules that contain an indole core, which is a bicyclic aromatic ring system, and carbazole units. These compounds exhibit unique electronic, photophysical, and potentially optoelectronic properties, which makes them potential candidates in various fields, including materials science and organic electronics.[71–73] Indolocarbazole cyanostilbenes combine both indolocarbazoles and cyanostilbenes, resulting in a hybrid structure that may exhibit synergistic properties. These compounds could potentially possess enhanced light-absorption capabilities, efficient charge transport characteristics, and tunable emission properties, which makes them intriguing candidates for applications in organic solar cells, organic light-emitting diodes (OLEDs), and other optoelectronic devices. The exploration and design of novel materials like indolocarbazole cyanostilbenes illustrate the continuous efforts to tailor molecular structures for specific electronic and photophysical behaviors, with the ultimate aim of advancing technology in fields ranging from energy generation to display technologies.

In 2013, Yang *et al.* developed two novel indolo[3,2-*b*]carbazole derivatives, **2** and **3** (Fig. 3), using the indolo-[3,2-*b*]carbazole unit as the electron donor and the –CN group as the electron acceptor unit; **2** and **3** show remarkable AIEE activity.[74] Both compounds possess the same π-conjugated core structure, but they differ in the stilbene group that has been substituted with the cyano, leading to similar optical characteristics and energy band gaps as well as strong charge transfer ability. Compounds **2** and **3** displayed poor emission in solution due to the presence of several non-radiative pathways, and exhibited strong emission in the aggregated state (AIEE). The authors proposed that the mechanism of fluorescence enhancement was *via* the large cyano group connected to a vinylene moiety creating intramolecular co-planarity and inhibiting the π–π stacking of molecules, which allows them to form nanoaggregates, and thus increases the emission. Further, the cyano group contributes significantly to the development of J-type aggregation, which is beneficial for the emergence of AIE and/or AIEE characteristics. The numerous intermolecular hydrogen bonds in compound **3** limit intramolecular vibration and rotation, as shown by crystallographic evidence, allowing compound **3** to emit brightly in the solid state. Furthermore, under favourable conditions, cyano groups provide enhanced formation of self-assembly for **2**. The molecules of **2** self-organize into one-dimensional ordered microfibers and/or nanorods that exhibit a notable optical waveguide with various water fractions, demonstrating that the aqueous suspension of microfibers favours fluorescence emission. These results proved that the molecular structure and aggregate packing of the novel indolo[3,2-*b*]carbazole derivatives have a significant impact on their AIEE capabilities.

Later, in 2021, the same research group synthesized four novel indolo[3,2-*b*]carbazole and cyanostilbene (**4–7**)[75](Fig. 4) based donor–acceptor conjugates with different substitutions by incorporating two α-cyanostilbene groups into the indolo-[3,2-*b*]carbazole unit with an A–π–D–π–A structure, which exhibited excellent photophysical properties in both the solution and aggregated states. All four compounds exhibited obvious ICT character and positive solvatochromism. The photophysical characteristics of all the compounds in various solvents, their aggregation emission nature, and solid state behavior were systematically examined. Compounds **4** and **6** displayed AIEE properties in a solution of THF/$H_2O$ (Fig. 5), and compounds **5** and **7** showed strong fluorescence emission in both solution and aggregated forms as a result of an increase in the degree of conjugation in solution and the absence of π–π stacking in the aggregated state. In addition, compound **4** demonstrated mechanically induced emission enhancement properties, and compound **6** exhibited mechanofluorochromism, which was substantiated by powder XRD, SEM, and DSC. Compounds **5** and **7**, however, showed no discernible fluorescence change during grinding, leading to the conclusion that the F atoms altered the stacking structure of the molecules. This work provided insight into the creation of more mechanofluorochromic materials with high fluorescence emission in both solution and aggregated forms.

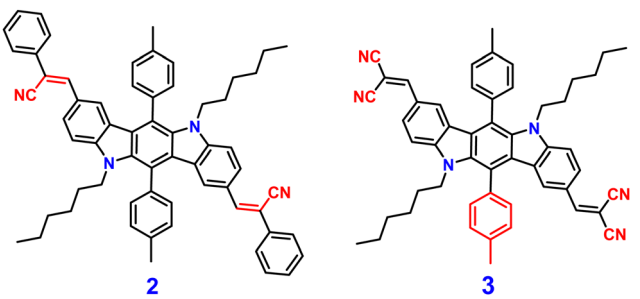


Fig. 3 Structure of compound **2** (left) and **3** (right).

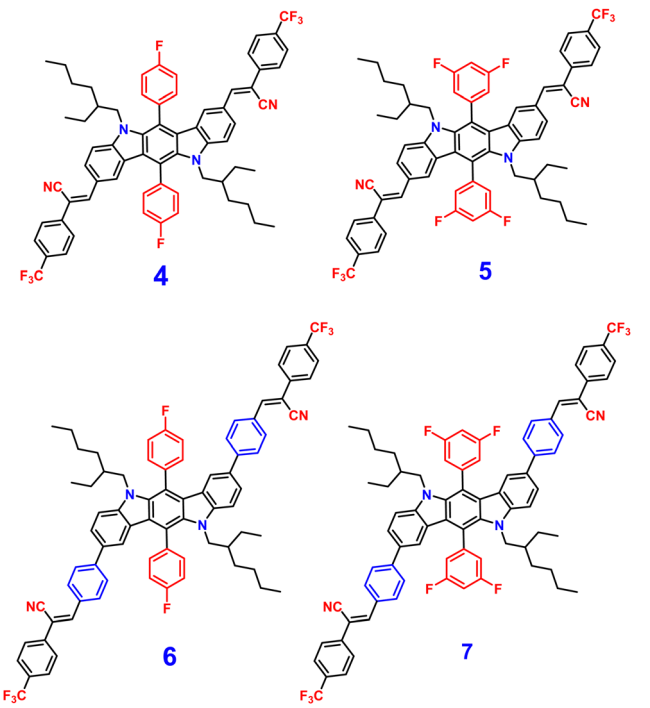


Fig. 4 Structure of compounds **4–7**.


This journal is © The Royal Society of Chemistry 2024

Open Access Article. Published on 04 January 2024. Downloaded on 7/20/2025 3:37:24 PM. This article is licensed under a Creative Commons Attribution-NonCommercial 3.0 Unported Licence.

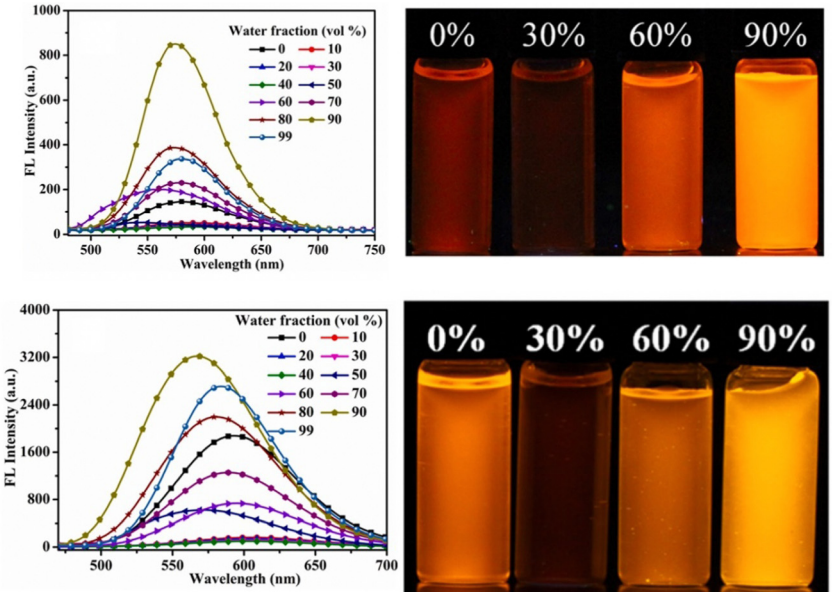


Fig. 5 Fluorescence spectra of compounds **4** and **6** with different fractions of water (left), and the corresponding images under 365-nm UV light (right). Reproduced with permission from ref. 75. Copyright 2021 Elsevier.

Recently, in the year 2022, they developed four novel indolo carbazole cyanostilbenes (**8–11**) (Table 1 and Fig. 6) with different terminal functional groups.[76] All the cyanostilbenes displayed low fluorescence emission in various solvents, except for benzene. Due to the presence of similar π-conjugated core structures, all four compounds have the same solvatochromic effect. The primary cause of the aggregation-induced emission enhancement seen in all four compounds in tetrahydrofuran–water mixed solution is the deformed spatial structure of the cyanostilbene group, which effectively prevents intermolecular π–π stacking in the aggregated state. Further, the compounds displayed an intramolecular charge transfer pathway from the indolocarbazole group to the cyanostilbene groups, which was demonstrated by DFT calculations as well as solvent-dependent studies. MFC characteristics were shown by molecules **9** and **11**, whose solid-state emission changed colour from green to yellow and yellow to yellow-orange, respectively (Fig. 7). The fluorescence red-shift was caused by the stacking patterns changing from the crystalline to amorphous states, as confirmed from single crystal data, powder XRD, SEM, and DSC. However, similar to the previous report in this case, the authors also claimed that the fluorine atom played a crucial role in the MFC characteristics.

Table 1 Photophysical parameters of carbazole–cyanostilbene derivatives (**1–17**)

| | $\lambda_{abs}$ (nm) | $\lambda_{em}$ (solution) (nm) | $\lambda_{em}$ (solid) | | | $\phi_f$ solid (%) | Ref. |
|---|---|---|---|---|---|---|---|
| | | | Pristine | Ground | Fumed | | |
| **1** | 365 | 497 | — | — | — | — | 70 |
| **2** | 410 | 499 | — | — | — | — | 71 |
| **3** | 460 | 559 | — | — | — | — | 71 |
| **4** | 424 | 544 | 508 | 536 | 508 | 19.1 | 75 |
| **5** | 419 | 533 | — | — | — | 17.43 | 75 |
| **6** | 421 | 602 | 548 | 572 | 548 | 22.72 | 75 |
| **7** | 420 | 590 | — | — | — | 9.21 | 75 |
| **8** | 338 | 436 | 536 | 542 | — | 17.53 | 76 |
| **9** | 338 | 436 | 521 | 554 | — | 8.31 | 76 |
| **10** | 337 | 434 | 527 | 531 | — | 17.10 | 76 |
| **11** | 338 | 436 | 551 | 592 | — | 5.80 | 76 |
| **12** | 426 | 560 | 540 | 560 | 540 | — | 80 |
| **13** | 440 | 585 | 582 | 609 | 582 | — | 80 |
| **14** | 371 | 590 | 485 | 524 | 485 | — | 81 |
| **15** | 347 | 604 | 479 | 534 | 479 | — | 81 |
| **16** | 431 | — | 526 | 606 | 526 | — | 81 |
| **17** | 410 | 640 | 566 | 598 | 570 | 81 | 82 |

## 9. Cruciform-shaped carbazole cyanostilbene derivatives

A cruciform luminophore is a molecule or compound that exhibits strong luminescence (light emission) in the solid state and displays a cross-like or cruciform shape. The unique cruciform structure of these luminophores can lead to interesting photophysical properties, such as enhanced light emission and tunable energy levels.[77–79] These luminophores are often used in various applications, including organic light-emitting diodes (OLEDs), fluorescent probes in biological imaging, and optoelectronic devices. In OLEDs, cruciform luminophores can be incorporated into the emissive layer to create displays with improved color purity and efficiency. Their structure allows for efficient charge transport, resulting in brighter and more vibrant displays. Further, their distinct shape can enable better spatial resolution and accuracy in imaging experiments. Overall, the unique structure and luminescent properties of cruciform luminophores make them promising candidates for various technological and scientific advances.

Carbazole and cyanostilbene conjugates displaying a cruciform architecture have been developed, in which the different

Open Access Article. Published on 04 January 2024. Downloaded on 7/20/2025 3:37:24 PM.
This article is licensed under a Creative Commons Attribution-NonCommercial 3.0 Unported Licence.

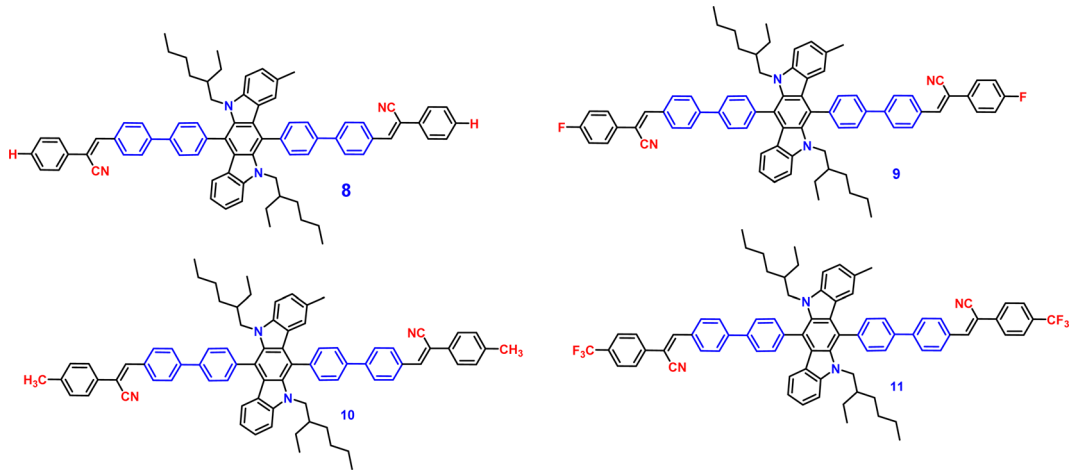


Fig. 6 Structure of compounds **8–11**.

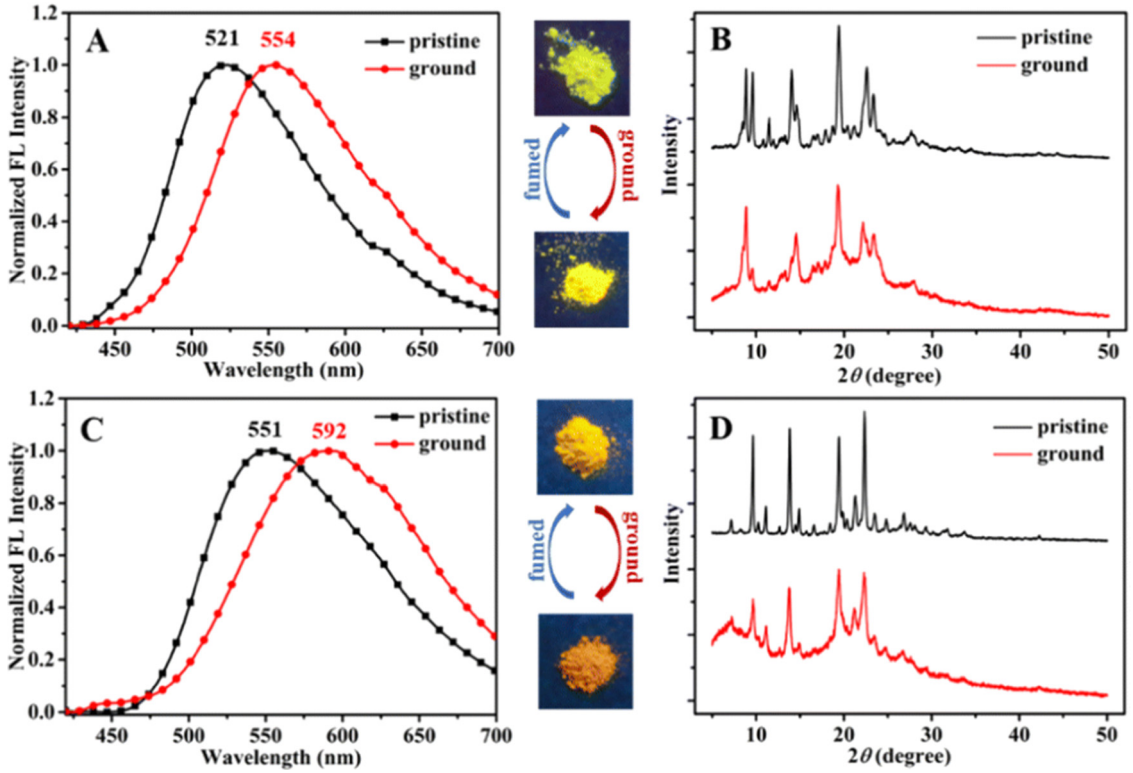


Fig. 7 Fluorescence spectra (A) and (C) and powder XRD patterns (B) and (D) of compounds **9** and **11**, respectively. Inset: Fluorescence images under 365 nm UV light. Reproduced with permission from ref. 75. Copyright 2022 Royal Society of Chemistry.

functional groups (carbazole and cyanostilbene) are positioned at the ends of the arms of the cross. On combining the carbazole and cyanostilbene in a cruciform, a molecule with a distinct structural arrangement is formed, which leads to interesting photophysical properties, including enhanced light emission and charge transport characteristics.

Liu *et al.* developed two twisted π-conjugated cruciform luminophores, **12** and **13** (Fig. 8), which were characterized by a rigid X-shaped geometry with two conjugated donors and acceptors intersecting at the central aromatic core in 2017.[80] These luminophores exhibit strong ICT properties with prominent AIE properties (AIE enhancement for **12** and **13** = 43 and 239, respectively), noteworthy luminescence mechanochromism properties (spectral shift for **12** and **13** = 42 and 49 nm, respectively), and excellent solid-state efficiency (up to 0.69 and 0.95, for **12** and **13**, respectively) (Table 1). The luminophore

 This journal is © The Royal Society of Chemistry 2024

Open Access Article. Published on 04 January 2024. Downloaded on 7/20/2025 3:37:24 PM.
This article is licensed under a Creative Commons Attribution-NonCommercial 3.0 Unported Licence.

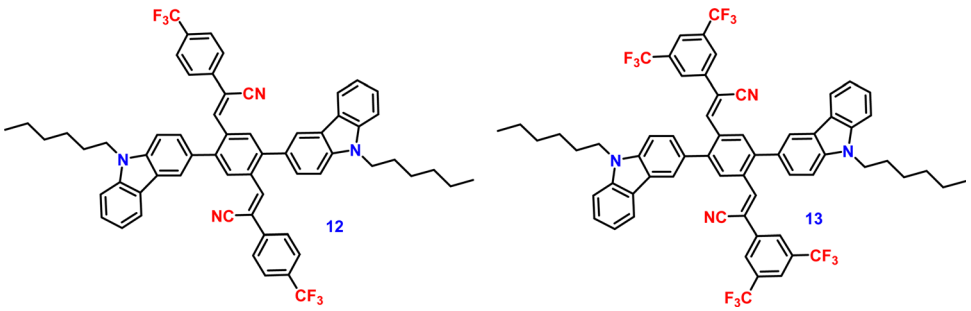


Fig. 8 Structure of compounds **12** and **13**.

3,5-bis(trifluoromethyl)phenyl with two trifluoromethyl groups bonded at the meta positions causes a much larger spatial hindrance, which allows **13** to have a more twisted spatial conformation, leading to more effective solid-state fluorescence, more obvious AIE, and more contrasting MFC behaviour than **12**. The reversible mechanochromism behavior of the luminophores was proved by the pXRD analysis, and the data suggests that the MFC behavior was caused by the transition between the crystalline and amorphous states (Fig. 9). Theoretical calculations and spectral analysis revealed that the two cross-conjugated compounds displayed a singular intramolecular charge-transfer (ICT) process in the excited state from the donor (carbazole) to the acceptor (dicyanodistyrylbenzene) axis.

In the following year, 2018, the same research group developed three donor–acceptor-containing cruciform luminophores, **14–16** (Fig. 10), with twisted molecular conformations.[81] The cross conjugated D–A compounds displayed distinctive intramolecular charge transfer (ICT) characteristics. The three cruciforms **14**, **15** and **16** have clearly apparent AIE properties, as well as high solid-state fluorescence quantum yields of 0.33, 0.42, and 0.49 and AIE factors of 9, 19, and >492, respectively. These changes were consistent with the degree of the torsional molecular spatial conformations induced by the steric hindrance between carbazole and substituted cyanostyryl, as well as the ICT degrees of the three compounds. The solid-state emission studies showed that grinding and DCM fuming treatment could change the fluorescence colour of the materials reversibly between bright blue-green (485 nm), bright blue-green (479 nm), bright yellow (526 nm), and light yellow-green (524 nm), yellow-green (534 nm), and orange-red (606 nm), resulting in large spectral red-shift values of 39, 55, and 80 nm for **14**, **15** and **16**, respectively (Table 1). The planarization of the molecular conformation and subsequent planar intramolecular charge transfer (PICT) under the influence of external force stimuli resulted in an increase in the

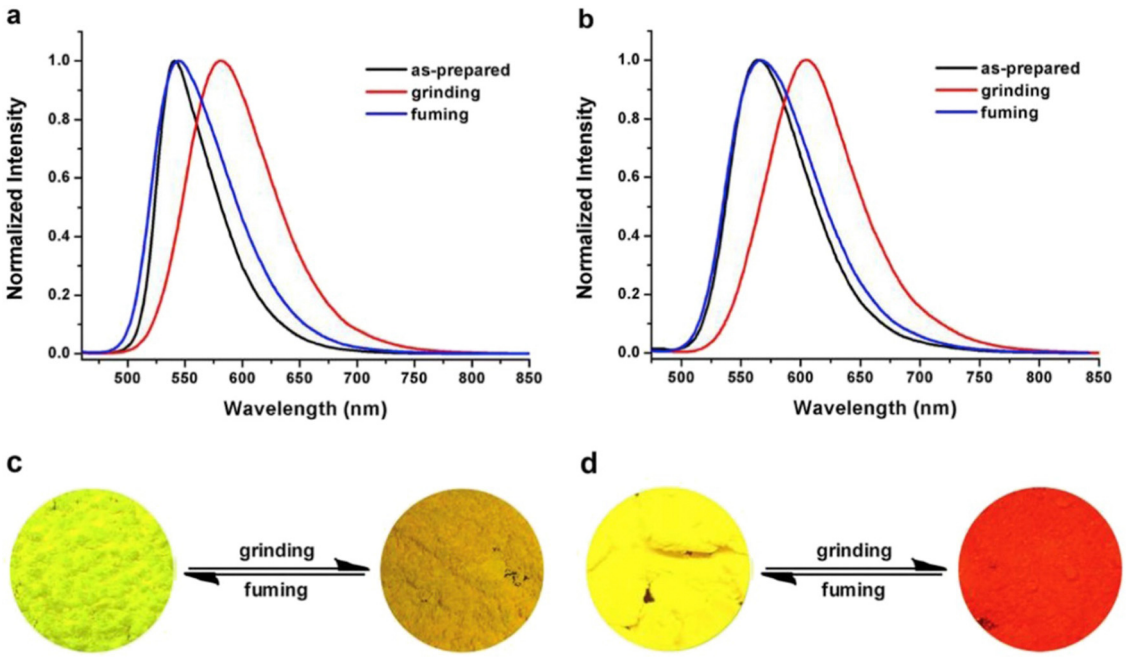


Fig. 9 Normalized fluorescence spectra of compound **12** (a) and compound **13** (b) excited at 450 nm in different solid-state conditions: as-prepared, ground and fumed. Photographs of the color changes of compound **12** (c) and compound **13** (d) under grinding and fuming. Reproduced with permission from ref. 80. Copyright 2018 Elsevier.

Open Access Article. Published on 04 January 2024. Downloaded on 7/20/2025 3:37:24 PM.
This article is licensed under a Creative Commons Attribution-NonCommercial 3.0 Unported Licence.

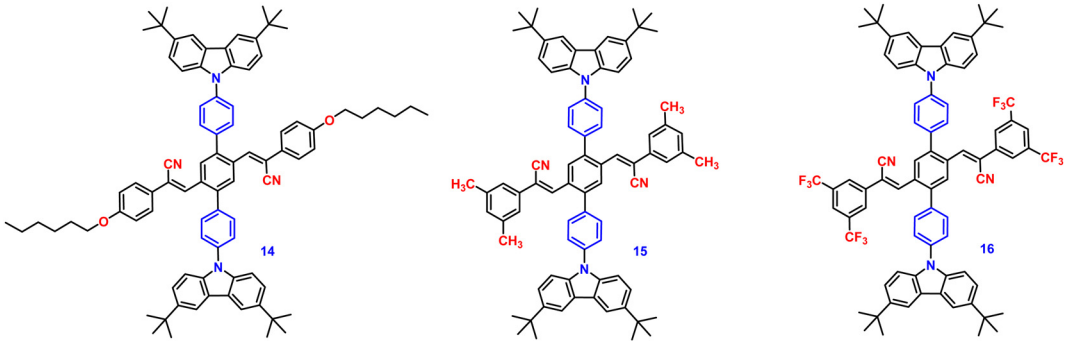


Fig. 10 Structure of compounds **14–16**.

MFC activities of the three compounds in the sequence **14** < **15** < **16**.

In 2019, the authors designed and synthesized another new cruciform, **17** (Fig. 11), containing an electron-donor carbazole unit and electron-acceptor dicyanovinylbenzene.[82] The photophysical properties in solution and the solid states based on the influence of electronic and steric effects were investigated. The distinctive structure gives the molecule a significantly deformed spatial conformation and an obvious ICT process, which was confirmed *via* solventdependent studies. The luminogen **17** displays AIE behaviour, exhibiting a high AIE of 405, and a high solid-state luminescence efficiency of up to 0.81 (Table 1). Additionally, it exhibits outstanding mechanofluorochromic (MFC) characteristics, with its solid-state emission changing from 566 nm to 598 nm upon grinding. The fact that the grinding-induced variations in fluorescence emission can be reversed by solvent-fuming and recovered by grinding suggests that the switching processes are extremely reversible, which was supported by the *p*-XRD and DSC analysis (Fig. 12). According to the PXRD studies, the crystalline–amorphous phase transformation between the initial and ground states is responsible for the MFC mechanism of the luminogen. The extension in molecular conjugation brought on by the planarization of the molecular conformation and subsequent planar intramolecular charge transfer (PICT) mechanism is the cause of the red-shift in the PL spectra after grinding.

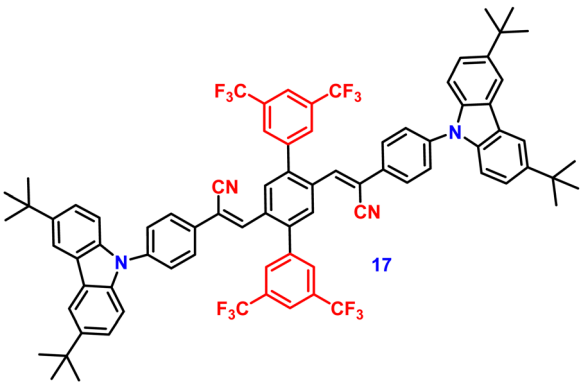


Fig. 11 Structure of compound **17**.

## 10. Carbazole–cyanostilbene derivatives with different terminal substitutions

Wang and co-workers synthesized five novel carbazole and cyanostilbene conjugates (Fig. 13) with different terminal substitutions in the year 2016.[83] These compounds displayed the usual properties of ICT, AIE, and CIEE, including great thermal stability ($T_d$ of up to 408 °C), high crystalline state efficiency (up to 77%) and strong thermal stability. It was demonstrated that by merely changing the electron acceptor (donor), their emission could be changed from blue to orange. In agreement with their respective emission maxima of 452, 515, 575, 462 and 469 nm, the emission spectra of the powders of **18a** (H), **18b** ($OCH_3$), **18c** ($NO_2$), **18d** ($CH_3$), and **18e** (Cl) clearly displayed tunable emission colour from blue to orange (Table 2). The hydrogen- (**18a**), methyl- (**18d**), and chlorine-substituted (**18e**) derivatives also showed remarkable reversible mechanochromic features (with emission wavelength changes of up to 119 nm), whereas the methoxyl (**18b**) and nitryl-substituted (**18c**) derivatives do not, due to their high crystallinity. The X-ray crystal structure study demonstrated that the stator–rotor designs, twisted conformations, and crystal packing modes were related to the AIE, CIEE-active, and mechanochromic behaviour. The density functional theory calculations also showed that the energy gaps of the fluorophores gradually decreased as the substituents' electron-donating or -accepting capacities increased, illuminating the substituent effect of the organic fluorophores on their photophysical properties.

In 2022, Xue *et al.* designed and synthesized two D–A carbazole and cyanostilbene (**19** and **20**)[84] (Fig. 14) conjugates to study the effects of the terminal group on the photophysical and mechanofluorochromic (MFC) abilities in solution and crystal state. The two designed molecules both have carbazole and cyanostilbene as the electron-donating and -withdrawing groups, respectively, and were functionalised with different terminal groups such as *t*-butylphenyl and naphthyl to understand the effect of the photophysical properties and were compared. It was found that, despite the presence of significantly aromatic naphthalene in **20**, a large steric barrier between the naphthalene and cyano results in a more twisted conformation and less π-conjugation compared to **19**. Both

 This journal is © The Royal Society of Chemistry 2024

Open Access Article. Published on 04 January 2024. Downloaded on 7/20/2025 3:37:24 PM.
This article is licensed under a Creative Commons Attribution-NonCommercial 3.0 Unported Licence.

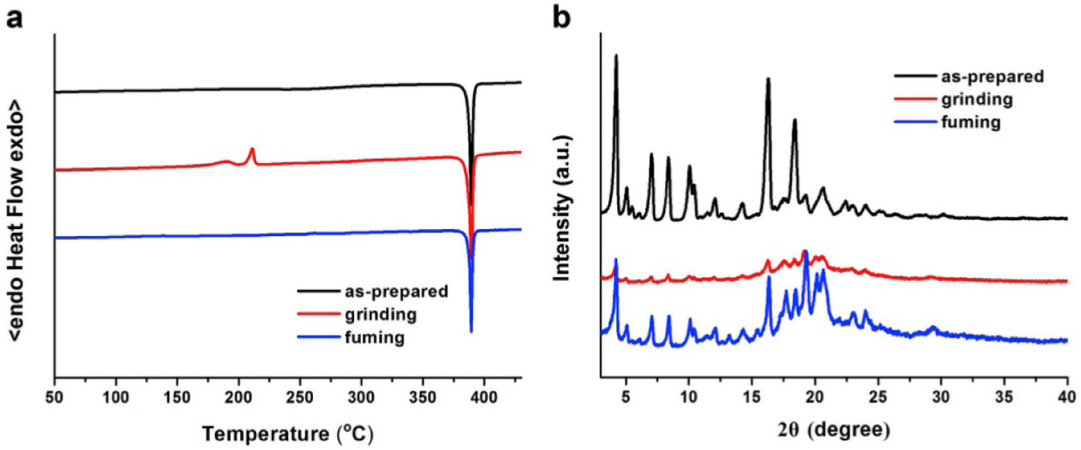


Fig. 12 DSC curves (a) and PXRD patterns (b) of compound **17** in different solid-state conditions: as-prepared, ground and fumed. Reproduced with permission from ref. 82. Copyright 2020 Elsevier.

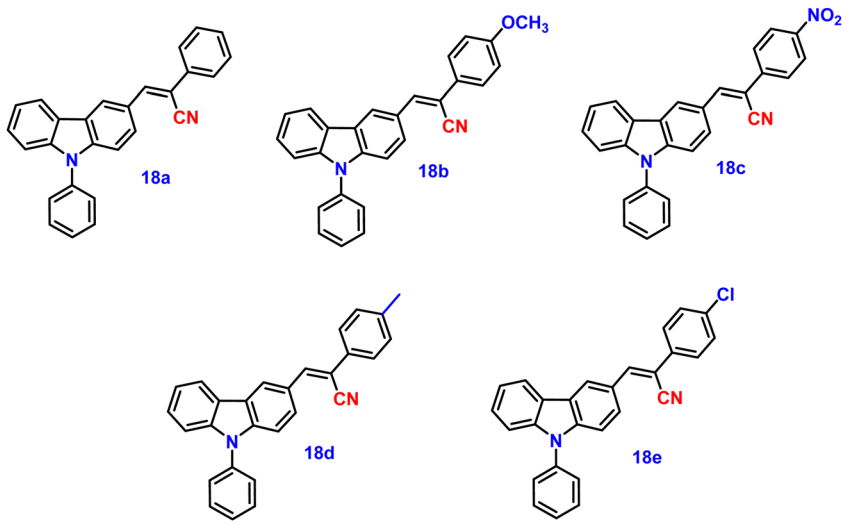


Fig. 13 Structure of compounds **18a–e**.

compounds have the same absorption and emission spectra, but their stacking pattern in the crystals are different, and they show different emission abilities in the solid state. Molecule **19** forms a one-dimension bimolecular array, while **20** forms dimers in crystals with strong π-stacking, which causes emission at longer wavelength as compared with that of **19**. The two compounds also show reversible mechanofluorochromic behaviours, and the spectral shift of **19** is greater than that of **20** due to a more distinct molecule planarization. However, their crystals strongly fluoresce blue, and the $\phi_f$ values for **19** and **20**, are 56% and 49%, respectively (Table 2), indicating that they exhibit crystallization-induced emission enhancement (CIEE) behaviour.

Recently, in 2023, Suneesh *et al.* created a series of 9-butyl-9H-carbazole derivatives[85] that exhibit strong solid-state emission with $-CF_3$ groups at various substituent positions of the phenyl group **21a–d**, which have no, *ortho*, *meta* and *para* trifluoromethyl substitution, respectively (Fig. 15). The synthesised luminogens were endowed with distinctive photophysical properties by the introduction of the $-CF_3$ group at the various substitution sites. The fluorinated derivatives exhibit intense solid-state emission as compared to the unsubstituted one because of the structural stiffness caused by the N–H and H–F supramolecular interactions. Compounds show dependence on the $-CF_3$ substitution position, and display impressive aggregation-induced emission (AIE), solvatofluorochromism, and mechanofluorochromic (MFC) features. The derivative with *ortho* substitution exhibits improved charge transfer characteristics and a peculiar dual-state fluorescence emission, which were employed for data encryption and anti-counterfeiting applications (Fig. 16). The derivative with the *p*-substitution has switchable MFC characteristics and a higher solid-state fluorescence quantum yield of 88% compared to the other derivatives. The mechanism of the reversible mechanofluorochromic characteristics was explained by PXRD and fluorescence lifetime studies.

Open Access Article. Published on 04 January 2024. Downloaded on 7/20/2025 3:37:24 PM.
This article is licensed under a Creative Commons Attribution-NonCommercial 3.0 Unported Licence.

Table 2 Photophysical parameters of carbazole–cyanostilbene derivatives **18–36**

| | $\lambda_{abs}$ (nm) | $\lambda_{em}$ (solution) (nm) | $\lambda_{em}$ (solid) (nm) | | | $\phi_f$ solid (%) | Ref. |
|---|---|---|---|---|---|---|---|
| | | | Pristine | Ground | Fumed | | |
| **18a** | 372 | 439 | 452 | 507 | — | 77 | 83 |
| **18b** | 375 | 444 | 515 | — | — | 57.9 | 83 |
| **18c** | 413 | 562 | 575 | — | — | 57.8 | 83 |
| **18d** | 375 | 441 | 462 | 581 | — | 25.7 | 83 |
| **18e** | 380 | 451 | 469 | 579 | — | 73.6 | 83 |
| **19** | 356 | 433 | 454 | 480 | 454 | 56 | 84 |
| **20** | 355 | 434 | 454 | 469 | 454 | 49 | 84 |
| **21a** | 371 | 456 | 485 | — | — | 36 | 85 |
| **21b** | 366 | 488 | 483 | — | — | 51 | 85 |
| **21c** | 382 | 457 | 488 | — | — | 52 | 85 |
| **21d** | 386 | 463 | 475 | 490 | — | 88 | 85 |
| **22** | 400 | 487 | 553 | 543 | 553 | — | 86 |
| **23** | 429 | 539 | 555 | 573 | 555 | — | 86 |
| **24** | 409 | 482 | — | — | — | — | 87 |
| **25** | 428 | 513 | — | — | — | — | 87 |
| **26** | 429 | 520 | — | — | — | — | 87 |
| **27** | 377 | 502 | 531 | 557 | 531 | 50.7 | 88 |
| **28** | 400 | 516 | 552 | 576 | 552 | 85.1 | 88 |
| **29** | 389 | 466 | — | — | — | — | 89 |
| **29a** | 393 | 434 | — | — | — | — | 89 |
| **30** | 398 | 484 | — | — | — | — | 89 |
| **30a** | 403 | 508 | — | — | — | — | 89 |
| **31** | 370 | 452 | — | — | — | — | 89 |
| **31a** | 371 | 461 | — | — | — | — | 89 |
| **32** | 384 | 514 | 548 | — | — | — | 90 |
| **33** | 392 | 450 | 574 | — | — | — | 90 |
| **34** | 420 | 546 | 609 | — | — | — | 90 |
| **35** | 442 | 502 | 558 | — | — | — | 90 |
| **36** | 413 | 487 | 627 | — | — | — | 90 |

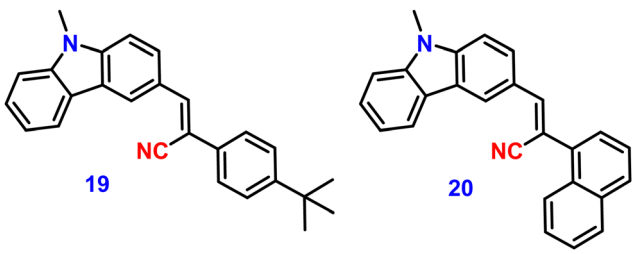


Fig. 14 Structure of compounds **19** and **20**.

This study offers a useful method for comprehending how the $-CF_3$ substitution position affects the luminescence characteristics of organic solids through fine-tuning of the molecular scaffolds.

## 11. Carbazole–cyanostilbene derivatives with D–π–A–π–D structures

Zhan *et al.* designed and synthesized two novel dumb-bell shaped D–π–A–π–D type cyanostilbene derivatives, **22** and **23** (Fig. 17) with two different donor groups, namely, carbazole and triphenylamine, respectively, in 2020.[86] The two compounds displayed distinctive ICT emission, clear AIE characteristics,

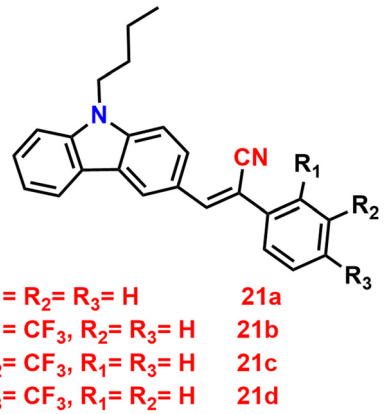


Fig. 15 Structure of compounds **21a–d**.

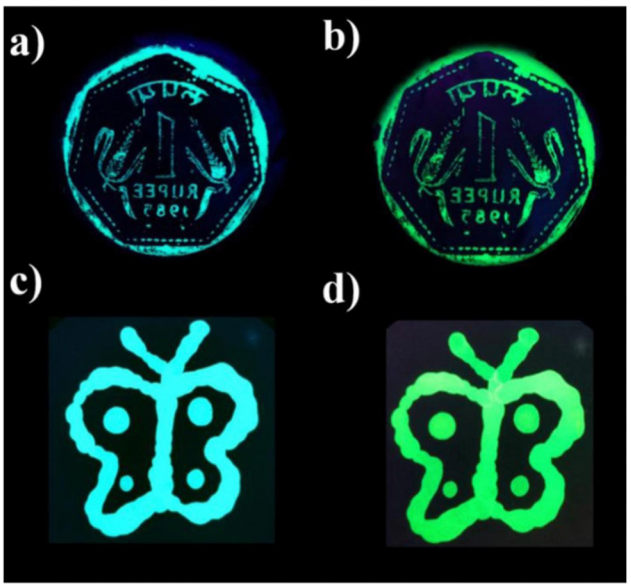


Fig. 16 (a) Data encryption of Indian 1-rupee coin on an aluminium foil using compound **21b** immersed in chloroform and dried. (b) The sealed coin after fuming with DMF. (c) Butterfly pattern drawn on a filter paper using chloroform solution of compound **21b** and dried. (d) The butterfly pattern after fuming with DMF. Reproduced with permission from ref. 85. Copyright 2023 Elsevier.

and strong fluorescence in the solid state. The solid-state fluorescence quantum efficiency data of the cyanostilbene derivatives **22** and **23** were established in order to objectively analyse their AIE properties. The $\phi_f$ values of the compounds are lower than 0.01 in diluted THF, while the $\phi_f$ in the solid state for **22** and **23**, increased to 0.31 and 0.42, respectively. It is interesting to note that the two molecules show different fluorescent responses towards pressure stimuli. While **23** displays a bathochromic shift of 18 nm after grinding, **22** displays an unexpected hypsochromic shift of 10 nm in the emission wavelength. The hypsochromic shift in the fluorescence wavelength of **22** may be due to poor π–π interaction and loose packing in the ground state, while the red-shifted mechanochromism of **23** may

 This journal is © The Royal Society of Chemistry 2024

Open Access Article. Published on 04 January 2024. Downloaded on 7/20/2025 3:37:24 PM.
This article is licensed under a Creative Commons Attribution-NonCommercial 3.0 Unported Licence.

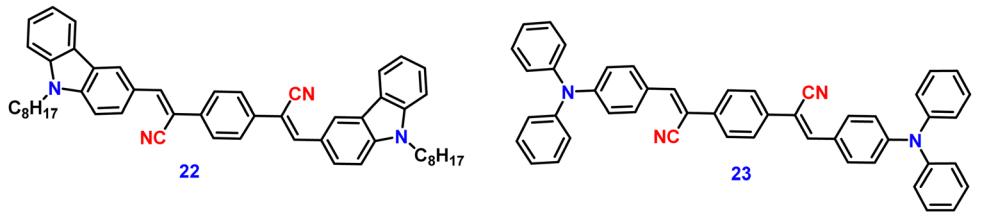


Fig. 17 Structure of compounds **22** and **23**.

be due to π–π stacking conversion from the H-aggregate to the J-aggregate under an external force. This finding was useful for making use of compounds with similar structures but different MFC properties.

In 2021, Tonga designed and synthesized three novel α-cyanostilbenes, **24–26** (Fig. 18), with a D–π–A–π–D structures containing different electron-donor groups, namely, carbazole, alkyldiphenylamine and dimethylamine.[87] By incorporating amino derivatives with cyanostilbene in the D–π–A–π–D structures, AIE luminogens with color-tunable emission ranging from green to yellow to red were obtained. Typically, an ICT process occurs in luminogens when electron-donating groups such as alkyldiphenylamine or carbazole are combined with electron-withdrawing groups like the cyano group. The alkyldiphenylamine and dimethylamine groups had greater electron-donor ability than the carbazole group, causing a red-shift of 20 nm in the emission spectra. Further, all compounds exhibited less emission in THF, but upon increasing the fraction of water, enhanced emission was observed (Fig. 19), which may result from the inhibition of twisted intramolecular charge transfer and *E*/*Z* isomerization. In particular, the emission was easily controlled by modifying the amino donor segments' *N*,*N*-alkyl/diphenyl and *N*,*N*-dimethyl substituents as well as the π-skeleton. Alkyl chains were used in **24** and **25** to provide a twisted conformation that allowed the molecules to exhibit AIE characteristics. The DFT results also showed that the degree of twisting significantly influences the colours of the aggregated state emission: like in the case of **24**, a substantial degree of twisting produced green emission and yellow emission in **25** and produced a red emission in **26**.

Yang *et al.* synthesized two novel D–π–A–π–D carbazole and cyanostilbene conjugates with different terminal groups, namely, **27** with an anilino group and **28** with an *N*,*N*-dimethylaniline group in 2022[88] (Fig. 20). The target compounds were synthesized through the Suzuki–Miyaura reaction and finally Knoevenagel condensation reaction, and were structurally characterized using $^{1}$H NMR,$^{13}$C NMR, FTIR, and ESI-MS analysis. Both compounds displayed an obvious ICT character, which is illustrated by the solvent-dependent studies. The two compounds have strong emission yields ($\phi_f$) of over 43% in solvents like toluene, ethyl acetate (EtOAc), and THF, and their average FL lifespan values in THF are 1.77 and 2.53 ns, accompanied by positive solvatochromism and substantial Stokes shifts. Compound **27** has longer absorption and FL wavelengths, as well as better FL quantum yields, when compared to **28**. The absorption and emission of **27** emerge at 377 and 502 nm, while those of **28** move to 400 and 516 nm. Compound **27** has a FL quantum yield ($\phi_f$) of 43.1%, whereas **28** has a value of 78.2% (Table 2). These findings suggest that one method for enhancing the photophysical characteristics of organic luminescent materials (OLMs) is to substitute an *N*,*N*-dimethylamino for the amino modification. Further, the authors utilised these compounds for the detection of picric acid (PA) (Fig. 21) and water traces in organic solvents, and the detection limits were determined to be 0.016% (**27**) or 0.040% (**28**) for water and 320 nM (**27**) or 538 nM (**28**) for PA. Additionally, with spectral shifts of over 24 nm, the two compounds show reversible mechanofluorochromism and also proved to be bright dual-state emission (DSE)-gens with multi-stimuli sensitive characteristics, making them intriguing

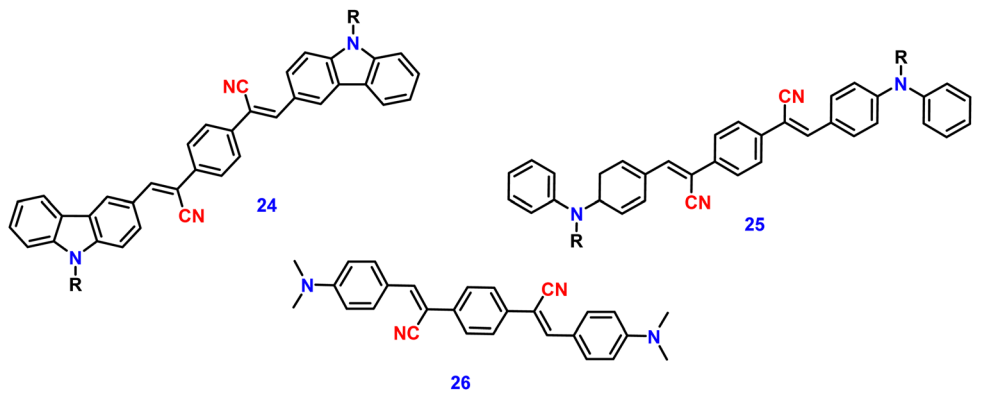


Fig. 18 Structure of compounds **24–26**.

Open Access Article. Published on 04 January 2024. Downloaded on 7/20/2025 3:37:24 PM.
This article is licensed under a Creative Commons Attribution-NonCommercial 3.0 Unported Licence.

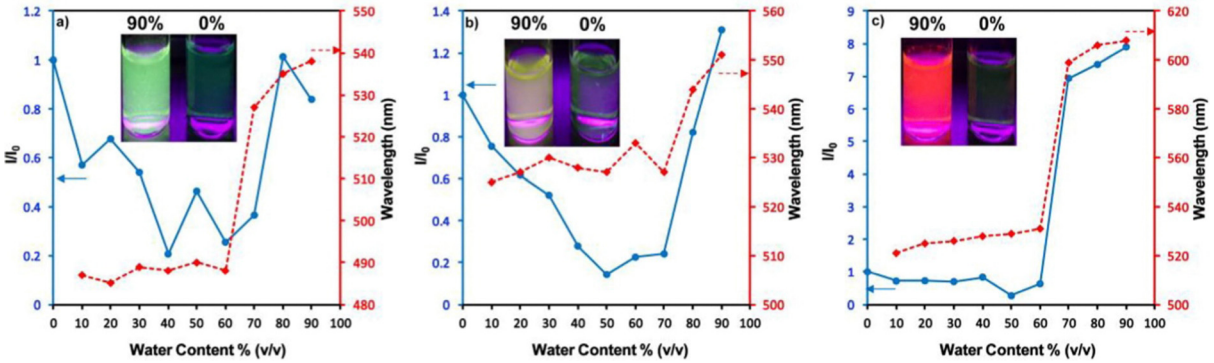


Fig. 19 Changes in the PL intensity and $k_{max}$ in THF–water mixtures with $f_w$ = 10–90%: (a) compound **24**, (b) compound **25** and (c) compound **26**. Inset: Fluorescence images of the luminogens in THF–water mixtures at $f_w$ = 90% and $f_w$ = 0% under illumination with a 365 nm UV lamp. Reproduced with permission from ref. 87. Copyright 2021 Elsevier.

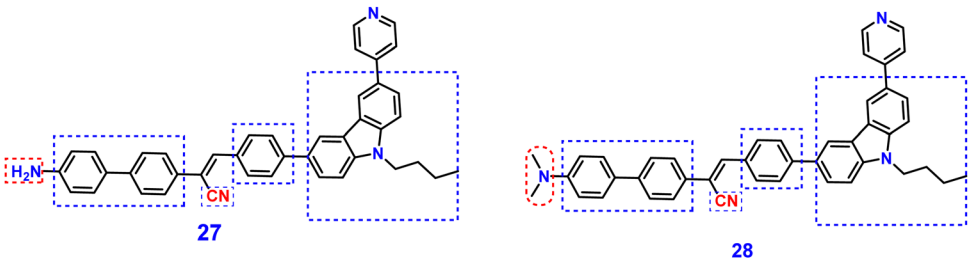


Fig. 20 Structure of compounds **27** and **28**.

materials for applications at both the molecular and aggregate levels.

## 12. Carbazole–cyanostilbene derivatives along with other amino derivatives

Kanvah *et al.* designed and synthesized a series of α-cyanostilbenes substituted with dimethylaniline, diphenylaniline and carbazole in 2014.[89] The authors developed six novel cyanostilbenes with these donor groups with a hydroxyl group and unsubstituted (Fig. 22). The photophysical properties of the novel stilbenes in various solvents, dioxane–water binary mixtures and the solid state were examined. The stilbenes with carbazole and triphenylamine donors exhibit distinct ICT character, which was confirmed by solvent-dependent studies. The absorption spectra of the hydroxyl-substituted stilbenes **29–31** show a modest (2–8 nm) blue shift in comparison to stilbenes **29a–31a**. The hydroxyl stilbenes show a higher quantum yield than their counterparts **29a–31a**, which was caused by the effect of the electron-donating nature of the hydroxyl group on the molecule. The usefulness of these compounds, especially stilbene **29**, as reversible pH probes was demonstrated by fluorescence experiments in a range of pH solutions. Stilbenes **29–31** exhibit significant fluorescence emission increase and bathochromic shift when water is utilised as the solvent medium. The aromatic ring of fluorophores **29–31** had a hydroxyl moiety, and also a dimethylamino group. They used compounds **29–31** as fluorescent probes for 'alkali' sensing (*via* phenolic OH) and 'acid' sensing (through the dimethylaniline group) due to their extraordinary emission behaviour in water.

In 2019, the same research group developed a series of pyridine-functionalized cyanostilbenes containing different amino group donors, namely carbazole–phenyl (**32**), *N*-ethyl carbazole (**33**), dimethylamino (**34**), julolidine (**35**) and triphenylamine (**36**), and the effect of the aggregation tendency was explored[90] (Fig. 23). The lowest absorption maximum of the compounds was observed for **32** with *N*-carbazole substitution, whereas the highest absorption maximum was observed for **35** with julolidine substitution. Due to the significant torsional distortion between the carbazole unit and phenyl group, there is a poor overlap of orbital contacts, which is responsible for the decreased absorption of **32**. Due to the improved planarity obtained from the direct conjugation of acrylonitrile with the third position of carbazole, the absorption of **33** is slightly red-shifted. The emission profiles of the compounds demonstrate favourable solvatochromic behaviour and provide evidence for intramolecular charge transfer (ICT) from the amino donor group to the electron-withdrawing cyano and pyridine units. The bulkiness of the donor substitution significantly affects the tendency of the acrylonitrile derivatives to aggregate. The compounds' AIE properties gradually decreased in the following order: **32** > **34** > **33** > **36** > **35** (Fig. 24). Due to effective

 This journal is © The Royal Society of Chemistry 2024

Open Access Article. Published on 04 January 2024. Downloaded on 7/20/2025 3:37:24 PM.
This article is licensed under a Creative Commons Attribution-NonCommercial 3.0 Unported Licence.

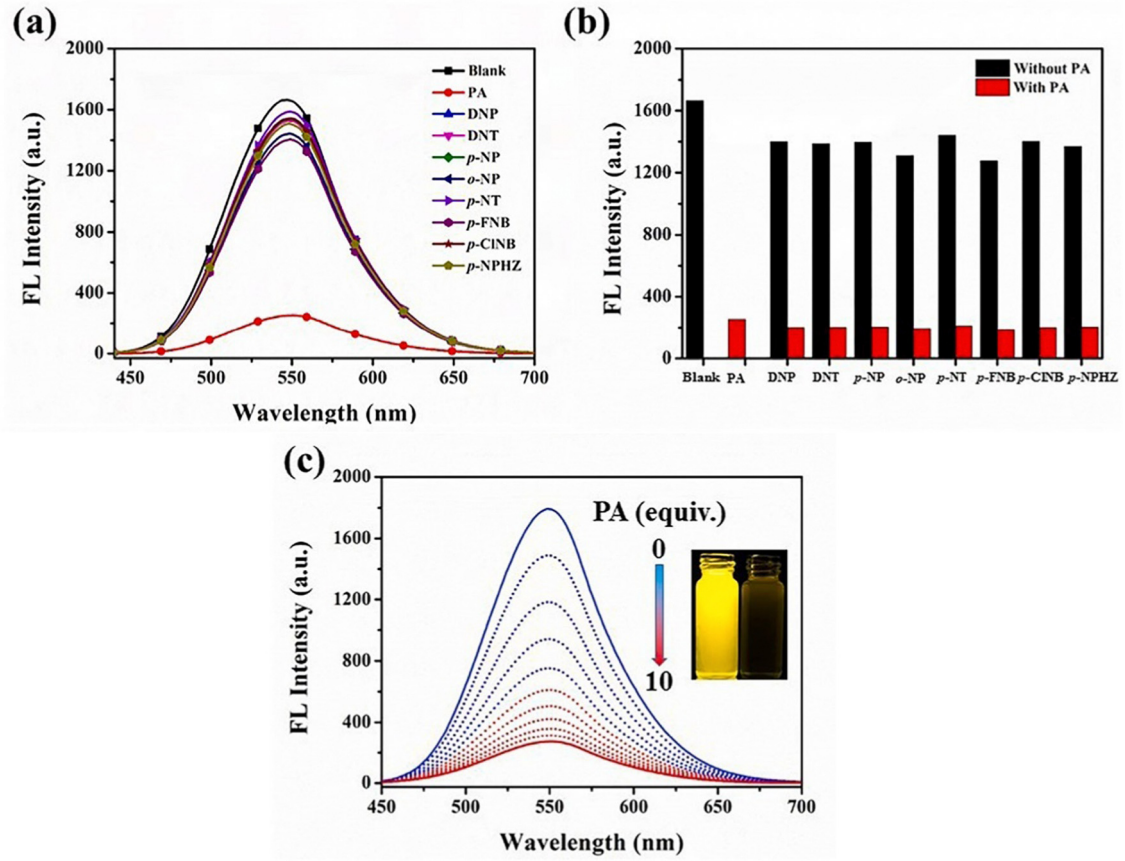


Fig. 21 (a) Fluorescence spectra of compound **27** in the presence of different analytes (10 equiv.). (b) Quenching percentage of compound **27** (10 μM) with analytes (10 equiv.) in THF before (black) and after (red) the addition of 10 equiv. of PA. (c) Fluorescence spectra of compound **27** in THF containing different amounts of PA. Inset: Photographs of compound **27** before (left) and after (right) PA addition under 365 nm UV exposure. Reproduced with permission from ref. 88. Copyright 2022 Elsevier.

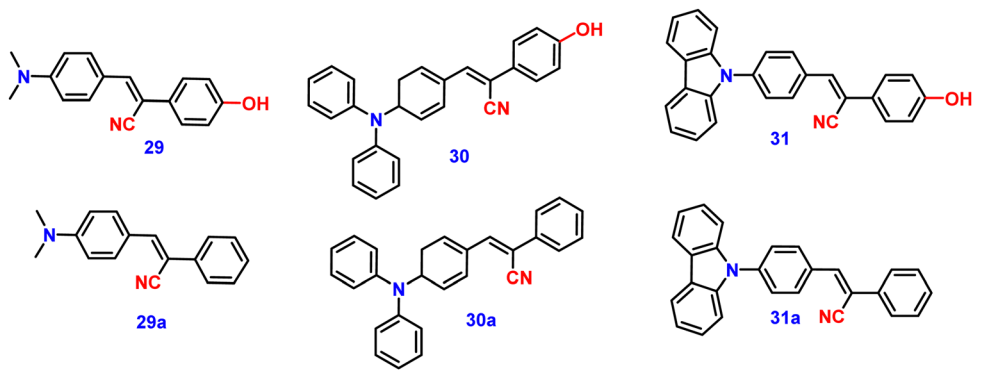


Fig. 22 Structure of compounds **29–31** and **29a–31a**.

interactions with nearby units, the carbazole unit and distal substitution of the cyano unit (**32**) produce a stronger AIE effect. The fluorescence lifetime decay profiles supported the development of aggregates and showed a correlation between the average lifetime and the stiffness of the molecular framework. The experimental findings were supported by the electron density distribution and projected DOS analyses of the compounds obtained using the DFT and TD-DFT methodologies. The redox characteristics of the compounds were investigated using cyclic voltammetry methods. A thorough picture of the morphology and hydrodynamic radii of the aggregates was produced using SEM and DLS investigations, respectively.

Open Access Article. Published on 04 January 2024. Downloaded on 7/20/2025 3:37:24 PM.
This article is licensed under a Creative Commons Attribution-NonCommercial 3.0 Unported Licence.

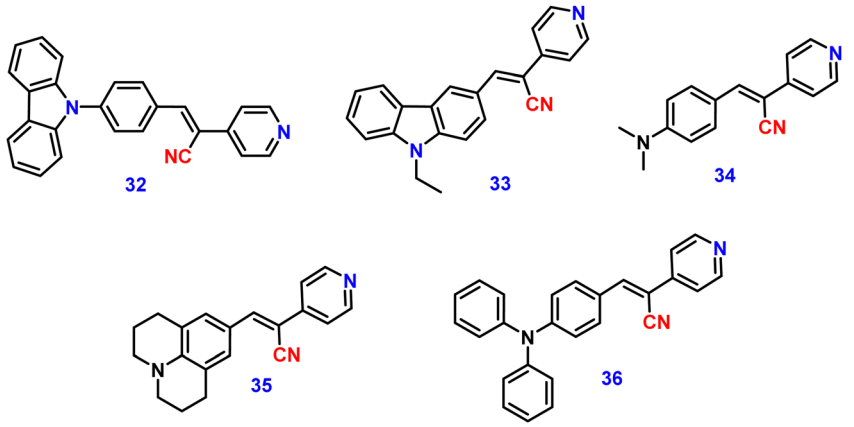


Fig. 23 Structure of compounds **32–36**.

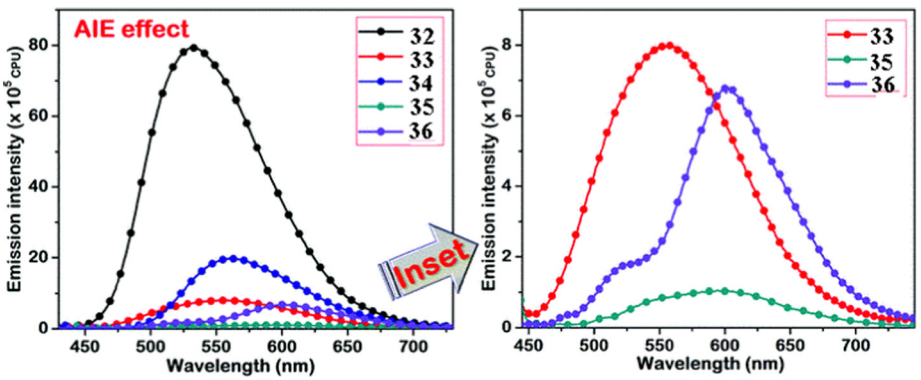


Fig. 24 AIE studies of the compounds **32–36** conducted in a dioxane–water binary solvent system. The inset represents the compounds with weak AIE characteristics. Reproduced with permission from ref. 90. Copyright 2020 Royal Society of Chemistry.

## 13. Some other examples of carbazole cyanostilbene derivatives

Jiang *et al.* created a biscyanovinyl diphenylcarbazole-based hexacatenar (**37**) in 2021, which was structurally characterised using $^{1}$H NMR, $^{13}$C NMR, and EA. The NH group served as the central core while cyanostilbene served as the functional group[91] (Fig. 25). They developed an efficient method for the rational construction of a number of novel luminous carbazole–cyanostilbene based conjugates. The mesophase behaviours, photophysical characteristics, photo-responsive behaviours, and AIEE effects of the luminogens were all carefully examined. The LC behaviour was shown to be substantially regulated by varying the chain length and temperature *via* POM, DSC, and XRD observations. When compared to the highest homologue, these lower homologues only self-organized into a rectangular columnar mesophase at lower temperatures and a hexagonal columnar mesophase at higher temperatures. The results of self-assembly showed that the creation of a Colrec/p2mm mesophase benefited from the presence of the carbazole unit and a long conjugated stiff core. These hexacatenars exhibit significant fluorescence in both solution and aggregation states, a specific solvatochromic effect, and AIEE characteristics. Additionally, in both the LC state and the solution state, these compounds demonstrated reversible photoresponsive characteristics. These design approaches opened a new route for producing

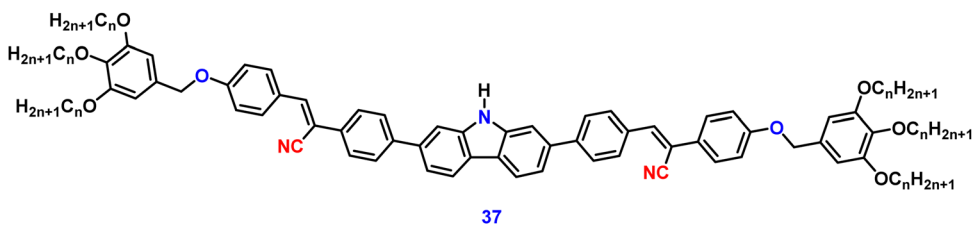


Fig. 25 Structure of compound **37**.

 This journal is © The Royal Society of Chemistry 2024

Open Access Article. Published on 04 January 2024. Downloaded on 7/20/2025 3:37:24 PM.
This article is licensed under a Creative Commons Attribution-NonCommercial 3.0 Unported Licence.

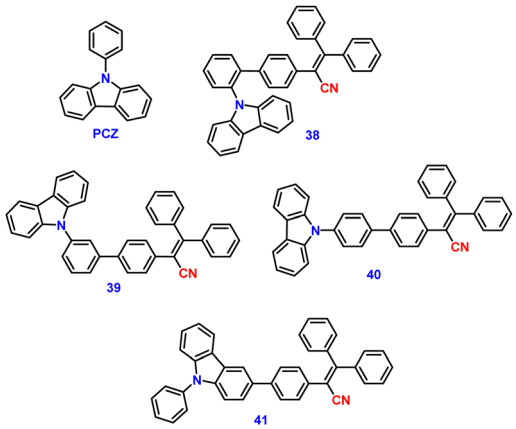


Fig. 26 Structure of compounds **38–41**.

functionalized AIE-active luminous LCs with intricate self-assembling architectures and photoresponsive behaviours.

Pie *et al.* designed and synthesized four novel triphenylacrylonitrile (TPAN)-adorned *N*-phenylcarbazoles (PCZ) (Fig. 26), which showed good aggregation-enhanced emission (AEE) characteristics in 2018.[92] The photophysical properties, including absorption, emission, and mechanochromism, are strongly influenced by the substituent position. All the luminogens

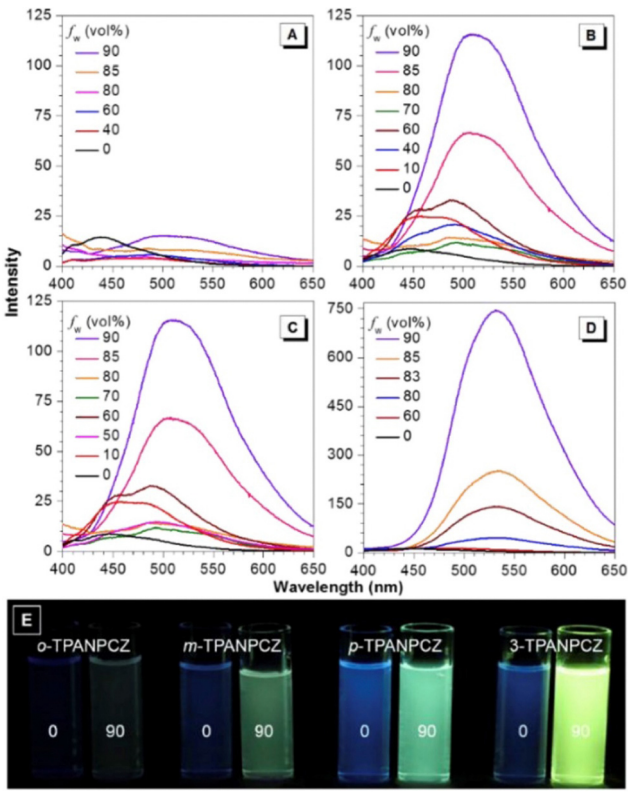


Fig. 27 Emission spectra of (A) compound **38**, (B) compound **39**, (C) compound **40** and (D) compound **41** in THF and THF/water mixtures with varying $f_w$ values. (E) Photographs of the luminogens in THF and a 10/90 THF/water mixture taken under 365 nm UV illumination. Reproduced with permission from ref. 92. Copyright 2018 Elsevier.

Table 3 Photophysical parameters of carbazole–cyanostilbene derivatives **37–43**

| | $\lambda_{abs}$ (nm) | $\lambda_{em}$ (solution) (nm) | $\lambda_{em}$ (solid) (nm) | | | $\phi_f$ solid (%) | Ref. |
|---|---|---|---|---|---|---|---|
| | | | Pristine | Ground | Fumed | | |
| **37** | 386 | 467 | — | — | — | — | 91 |
| **38** | 338 | — | 500 | 500 | 500 | 18.75 | 92 |
| **39** | 339 | — | 455 | 463 | 455 | 31.93 | 92 |
| **40** | 342 | — | 460 | 495 | 460 | 53.68 | 92 |
| **41** | 350 | — | 489 | 526 | 489 | 56.80 | 92 |
| **42a** | 375 | 509 | 514 | — | — | 63.4 | 93 |
| **42b** | 401 | 561 | 548 | 569 | 548 | 71 | 93 |
| **42c** | 378 | 525 | 537 | — | — | 93.9 | 93 |
| **42d** | 373 | 507 | 508 | — | — | 93.3 | 93 |
| **43a** | 404 | 473 | 477 | 554 | 477 | 28 | 42 |
| **43b** | 406 | 458 | 520 | 596 | 520 | 22 | 42 |
| **43c** | 410 | 450 | 523 | 610 | 523 | 18 | 42 |

demonstrate aggregation-enhanced emission (AEE) behaviour in THF/$H_2O$ (Fig. 27). For **38**, **39**, **40** and **41**, the $\phi_f$ values are as low as 1.61%, 0.96%, 0.78%, and 0.88% in solution; however, their $\phi_f$ values increase to 18.75%, 31.93%, 53.68%, and 56.80% under aggregate state (Table 3), from the results AEE factor calculated to be (AEE = $\phi_{f,asp}/\phi_{f,s}$) 11.6, 33.3, 68.8 and 64.5, respectively. Because of its more-active molecular movements in the solid state, **38** has a relatively low $\phi_{f,asp}$. All isomers except **38** exhibit different reversible luminous mechanochromism because of the breakdown and re-formation of their twisted conformations and intermolecular connections in the crystalline and amorphous states. The luminogens were used to fabricate OLEDs with $L_{max}$, $CE_{max}$, $PE_{max}$, and $EQE_{max}$ values of 2570 cd $m^{-2}$, 6.28 cd $A^{-1}$, 5.64 lm $W^{-1}$ and 2.60%.

In 2022, Ding and co-workers synthesized four novel carbazole-based cyanostilbenes with different terminal substitutions, *i.e.*, unsubstituted **42a**, **42b** with an *N*,*N*-dimethylamino group, **42c** with a cyano group, and **42d** with a $^t$Bu group (Fig. 28).[93] The influence of the electronic factors of the substituent groups on the photophysical properties was analysed. It is interesting to note that just one of the four molecules, **42b**, demonstrates dual-state emission (DSE) behaviour, whilst the other three molecules show normal AIE behaviour. **42b** exhibits greater molar absorption coefficients, longer FL and absorption wavelengths, and stronger FL intensity in the same solvent when compared to the other three compounds; this is due to the intensive ICT process originating from the strongly electron-donating *N*,*N*-dimethylamino group. The average FL lifespan values of the solids are 1.63, 1.82, 3.97, and 2.12 ns, and the fluorescence quantum yields of **42a**, **42b**, **42c** and **42d** are as high as 63.4%, 71.0%, 93.9%, and 93.3%, respectively (Table 3). Additionally, the authors showed that the compound **42b** can be utilised for the detection of water, picric acid (PA), and mechanofluorochromism (MFC) (Fig. 29). The results show how significantly the *N*,*N*-dimethylamino group improved the optical properties of fluorescent dyes. In the field of multi-parameter analysis for complicated environments, compound **42b** with DSE and multi-stimuli-sensitive qualities has many potential applications.

Very recently, in 2023, Swamy *et al.* designed and synthesized three novel carbazole–anthracene appended cyanostilbenes,

Open Access Article. Published on 04 January 2024. Downloaded on 7/20/2025 3:37:24 PM.
This article is licensed under a Creative Commons Attribution-NonCommercial 3.0 Unported Licence.

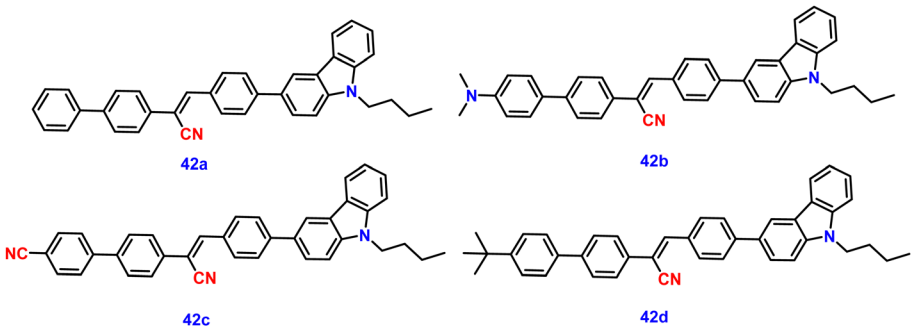


Fig. 28 Structure of compounds **42a–d**.

**43a–c**, with different terminal substitutions (Fig. 30).[42] The three cyanostilbenes differ from each other by a minor modification in the cyanostilbene unit, and the way in which these changes alter the photophysical properties was taken into account. The photophysical properties of the compounds in different solvents, as well as their aggregation induced emission and solid-state emission, were carefully studied. When the polarity of the solvent is increased, the compound with the electron-donating –OMe group exhibits reverse solvatochromism, whereas the other two compounds with –H substitution and the electron-withdrawing group –Cl exhibit positive solvatochromism (Fig. 31). This makes the fluorescence spectrum of compound **43a** wholly distinct from those of the other two compounds (**43b** and **43c**) and this observation is rare in the context of cyanostilbene derivatives. All three compounds displayed AIE behaviour in an ACN/$H_2O$ mixture. Moreover, all compounds display reversible mechanofluorochromism (MFC) properties, with the colour of compound **43a** changing from blue-green to green while the other compounds showed greenish-yellow to yellowish colour, which was further confirmed by powder XRD and solid-state emission data. The optimised ground state energy levels and experimental observations were validated by theoretical calculations. Furthermore, all compounds exhibit outstanding thermal stability and strong solid-state luminescence, which could be employed for OLED fabrication.

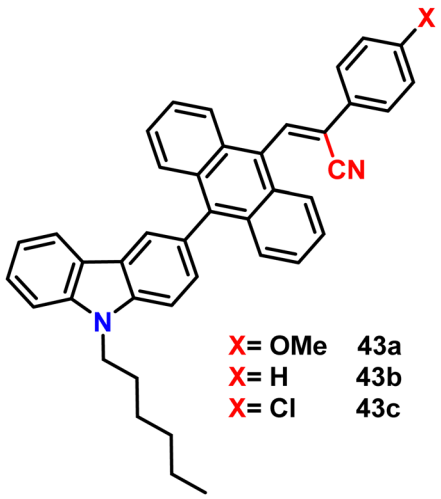


Fig. 30 Structure of compounds **43a–c**.

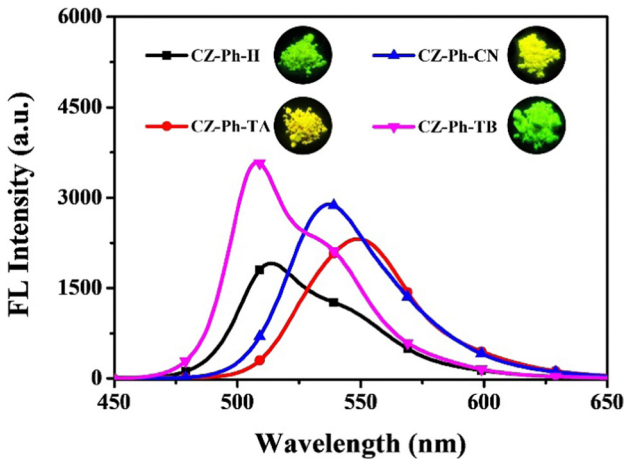


Fig. 29 FL spectra of the compounds in the solid state. Inset: Photographs of powders under 365 nm UV exposure. Reproduced with permission from ref. 93. Copyright 2022 Wiley.

## 14. Conclusions and future outlook

The journey through the world of carbazole-based cyanostilbenes, with their remarkable aggregation-induced emission (AIE) and mechanofluorochromism (MFC) characteristics, has unveiled a landscape of unparalleled luminescent potential. As we reflect on the structure, properties, and applications discussed in this review, it becomes evident that these molecules transcend traditional boundaries, illuminating new avenues for innovation in various domains. The quest to harness the AIE phenomenon has led researchers to the design and creation of luminophores that defy the conventional quenching effects of aggregation. The delicate balance of molecular structure, aggregation propensity, and energy states guides the remarkable transition from darkness to brilliance, thus revolutionizing optoelectronics, sensors, and beyond. In parallel, the exploration of mechanofluorochromism has unmasked the malleable nature of these molecules, which responding dynamically to mechanical stimuli and redefine responsive materials. From optoelectronic devices that emit vibrant light to stress-sensing

 This journal is © The Royal Society of Chemistry 2024

Open Access Article. Published on 04 January 2024. Downloaded on 7/20/2025 3:37:24 PM.
This article is licensed under a Creative Commons Attribution-NonCommercial 3.0 Unported Licence.

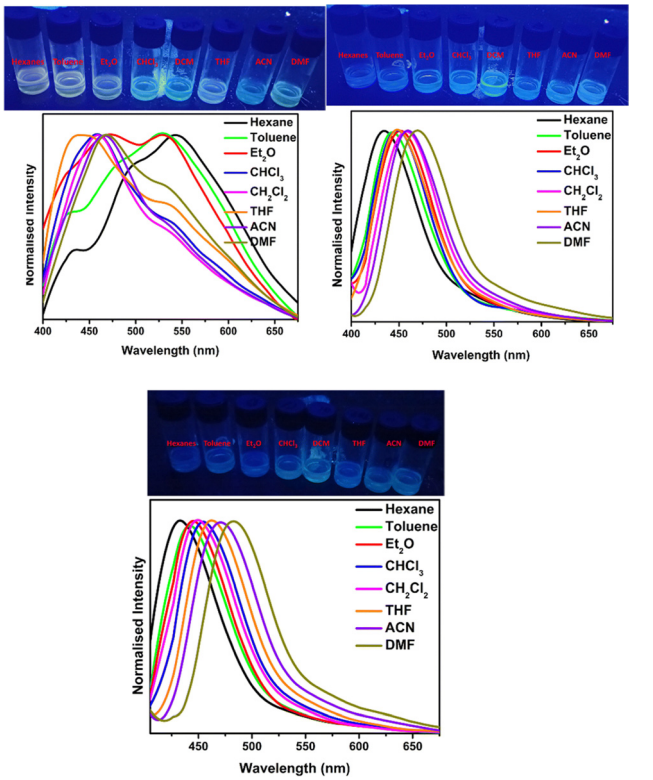


Fig. 31 The Fl spectra of compound **43a** (top left), **43b** (top right) and **43c** (bottom) at various solvents; inset: digital photos taken under 365 nm UV light. Reproduced with permission from ref. 42. Copyright 2023 Royal Society of Chemistry.

materials that visually communicate their surroundings, the applications of carbazole-based cyanostilbenes extend far and wide. They beckon us to envision adaptable displays, novel sensing platforms, and responsive coatings that capture the imagination of both researchers and industries alike. Yet, as we stand at this crossroads of discovery, we recognize that challenges lie ahead. The intricate interplay between molecular design and luminescence behavior demands a deeper understanding, urging us to unravel the mechanisms governing AIE and MFC. The pursuit of enhanced performance, extended lifetimes, and diverse applications invites further research into the uncharted territories of these compounds.

The carbazole-based cyanostilbenes have illuminated a path that extends far into the future, promising a landscape of transformative possibilities and uncharted horizons. As we look ahead, several key trends and directions emerge to guide the trajectory of research and innovation in this field. The future of carbazole-based cyanostilbenes lies in the precision of molecular design. Researchers will explore novel strategies to fine-tune AIE and MFC behaviors through controlled modifications of their chemical structures. The search for molecules with enhanced luminescence and responsiveness will propel innovation in synthesis techniques and theoretical modeling. In the field of optoelectronics, the integration of carbazole-based cyanostilbenes into cutting-edge devices is poised to accelerate. Their AIE properties open doors to brighter, more energy-efficient OLEDs and displays, transforming the visual experience for consumers. Harnessing MFC for stress-sensing applications in wearable electronics and smart materials will forge a new dimension of interaction between humans and technology. The connection of AIE and MFC will give rise to an era of responsive materials that adapt and communicate in response to their environment. From structural health monitoring to smart textiles, these materials will revolutionize industries, offering real-time feedback and visual cues that enhance safety, efficiency, and user experience. The future of carbazole-based cyanostilbenes transcends the boundaries of chemistry. The connections between chemists, materials scientists, engineers, and biologists will amplify the impact of these compounds. Synergies with fields like nanotechnology, bioimaging, and environmental monitoring will unveil unexplored dimensions of their application potential. As research advances, considerations of sustainability and green chemistry will take center stage. Developing synthesis methods that are efficient, cost-effective, and environmentally benign will be paramount. Eco-friendly approaches to manufacturing carbazole-based cyanostilbenes will align with the global pursuit of a greener future. Communicating the potential of AIE and MFC to a wider audience, fostering the curiosity of young minds, and encouraging multidisciplinary engagement will ensure that the brilliance of carbazole-based cyanostilbenes inspires generations to come. In essence, the future of carbazole-based cyanostilbenes is ablaze with the promise of innovation and impact. The fusion of AIE and MFC has ignited a beacon that guides researchers, creators, and visionaries toward novel applications, sustainable technologies, and a world illuminated by the boundless potential of these extraordinary molecules. As we navigate this path, we are poised to redefine possibilities in an era of transformative change.

In closing, the carbazole-based cyanostilbenes, with their dual advantages of AIE and MFC, beckon us to peer beyond the limits of conventional luminescence. Their radiance transcends the confines of molecules, sparking a beacon of possibilities that guides us toward more efficient, adaptive, and impactful technologies. As researchers and visionaries, we stand poised to capture this brilliance and etch it into the future of materials science, optoelectronics, and beyond.

## Abbreviations

| | |
|---|---|
| AIE | Aggregation-induced emission |
| AIEE | Aggregation-induced emission enhancement |
| ICT | Intramolecular charge transfer |
| TICT | Twisted intramolecular charge transfer |
| MFC | Mechanofluorochromism |
| OLED | Organic light-emitting diodes |
| OPVs | Organic photovoltaics |
| ACQ | Aggregation-caused quenching |
| SEM | Scanning electron microscope |
| THF | Tetrahydrofuran |
| PXRD | Powder X-ray diffraction |

Open Access Article. Published on 04 January 2024. Downloaded on 7/20/2025 3:37:24 PM. This article is licensed under a Creative Commons Attribution-NonCommercial 3.0 Unported Licence.

| | |
|---|---|
| DSC | Differential scanning calorimetry |
| DFT | Density functional theory |
| CIEE | Crystallization-induced emission enhancement |
| NMR | Nuclear magnetic resonance |
| FT-IR | Fourier-transform infrared spectroscopy |
| ESI-MS | Electrospray ionisation mass spectrometry |
| POM | Polarized optical microscopy |
| LC | Liquid crystal |
| DSE | Dual-state emission |
| LOD | Limit of detection |
| TD-DFT | Time-dependent density-functional theory |

## Conflicts of interest

The authors declare no competing financial interest.

## Acknowledgements

CAS P acknowledges the research grant SERB/EEQ/2021/000180 and NITC-FRG for financial support. A. A. thanks the National Institute of Technology, Calicut, for GATE-JRF fellowship.

## References

1 K. Li, T.-B. Ren, S. Huan, L. Yuan and X.-B. Zhang, *J. Am. Chem. Soc.*, 2021, **143**, 21143–21160.
2 S.-W. Zhang and T. M. Swager, *J. Am. Chem. Soc.*, 2003, **125**, 3420–3421.
3 L. Basabe-Desmonts, D. N. Reinhoudt and M. CregoCalama, *Chem. Soc. Rev.*, 2007, **36**, 993–1017.
4 N. Tessler, V. Medvedev, M. Kazes, S. Kan and U. Banin, *Science*, 2002, **295**, 1506–1508.
5 G. Niu, R. Zhang, J. P. C. Kwong, J. W. Y. Lam, C. Chen, J. Wang, Y. Chen, X. Feng, R. T. K. Kwok, H. H. Y. Sung, I. D. Williams, M. R. J. Elsegood, J. Qu, C. Ma, K. S. Wong, X. Yu and B. Z. Tang, *Chem. Mater.*, 2018, **30**, 4778–4787.
6 A. Kitai, *Luminescent Materials and Applications*, John Wiley Sons, Chichester, 2008.
7 S. Hudson and Z. M. Wang, *Acc. Chem. Res.*, 2009, **42**, 1584–1596.
8 K. Figueira-Duarte and T. M. Mullen, *Chem. Rev.*, 2011, **111**, 7260–7314.
9 Z. Li, Z. R. Li and H. Meng, *Organic light-emitting materials and devices*, CRC Press, 2006.
10 C. W. Tang and S. A. Vanslyke, *Appl. Phys. Lett.*, 1987, **51**, 913–915.
11 R. H. Friend, R. W. Gymer, A. B. Holmes, J. H. Burroughes, R. N. Marks, C. Taliani, D. D. C. Bradley, D. A. D. Santos, J. L. Brédas, M. Lögdlund and W. R. Salaneck, *Nature*, 1999, **397**, 121.
12 K. Mullen and U. Scherf, *Organic light emitting devices: synthesis, properties and applications*, 2006.
13 A. C. Grimsdale, K. L. Chan, R. E. Martin, P. G. Jokisz and A. B. Holmes, *Chem. Rev.*, 2009, **109**, 897–1091.
14 C. A. Strassert, C. H. Chien, M. D. G. Lopez, D. Kourkoulos, D. Hertel, K. Meerholz and L. D. Cola, *Angew. Chem., Int. Ed.*, 2011, **50**, 946–950.
15 I. D. W. Samuel and G. A. Turnbull, *Chem. Rev.*, 2007, **107**, 1272–1295.
16 C. Zhang, C.-L. Zou, Y. Yan, R. Hao, F.-W. Sun, Z.-F. Han, Y. S. Zhao and J. Yao, *J. Am. Chem. Soc.*, 2011, **133**, 7276–7279.
17 Z. Yang, A. Sharma, J. Qi, X. Peng, D. Y. Lee, R. Hu, D. Lin, J. Qu and J. S. Ki, *Chem. Soc. Rev.*, 2016, **45**, 4651–4667.
18 H. B. Cheng, Y. Li, B. Z. Tang and J. Yoon, *Chem. Soc. Rev.*, 2020, **49**(1), 21–31.
19 T. Jairam and W. P. Hon, *J. Mater. Chem. C*, 2022, **10**, 16173–16217.
20 X.-H. Zhu, J. Peng, Y. Cao and J. Roncali, *Chem. Soc. Rev.*, 2011, **40**, 3509–3524.
21 J. Tagare and S. Vaidyanathan, *J. Mater. Chem. C*, 2018, **6**, 10138–10173.
22 Y. Li, Y. Sun, Y. Zhang and W.-J. Dong, *Opt. Mater.*, 2020, **108**, 110194.
23 A. Bessette and G. S. Hanan, *Chem. Soc. Rev.*, 2014, **43**, 3342–3405.
24 J. Gierschner, J. Shi, B. Milián-Medina, D. Roca-Sanjuán, S. Varghese and S. Y. Park, *Adv. Opt. Mater.*, 2021, **9**, 2002251.
25 M. K. Bera, P. Pal and S. Malik, *J. Mater. Chem. C*, 2020, **8**, 788–802.
26 J. Mei, Y. Hong, J. W. Y. Lam, A. Qin, Y. Tang and B. Z. Tang, *Adv. Mater.*, 2014, **26**, 5429–5479.
27 Z. Wang, Y. Zhou, R. Xu, Y. Xu, D. Dang, Q. Shen, L. Meng and B. Z. Tang, *Coord. Chem. Rev.*, 2022, **451**, 214279.
28 Y. Sun, Z. Lei and H. Ma, *J. Mater. Chem. C*, 2022, **10**, 14834–14867.
29 R. T. Kwok, C. W. Leung, J. W. Lam and B. Z. Tang, *Chem. Soc. Rev.*, 2015, **44**, 4228–4238.
30 J. Luo, Z. Xie, J. W. Y. Lam, L. Cheng, H. Chen, C. Qiu, H. S. Kwok, X. Zhan, Y. Liu, D. Zhu and B. Z. Tang, *Chem. Commun.*, 2001, 1740–1741.
31 Y. Hong, J. W. Y. Lam and B. Z. Tang, *Chem. Soc. Rev.*, 2011, **40**, 5361–5388.
32 J. Mei, N. L. C. Leung, R. T. K. Kwok, J. W. Y. Lam and B. Z. Tang, *Chem. Rev.*, 2015, **21**, 11718–11940.
33 Y. D. Tu, J. Zhang, Y. Zhang, H. H. Y. Sung, L. Liu, R. T. K. Kwok, J. W. Y. Lam, I. D. Williams, H. Yan and B. Z. Tang, *J. Am. Chem. Soc.*, 2021, **143**, 11820–11821.
34 H. Wang, Q. Li, J. Zhang, H. Zhang, Y. Shu, Z. Zhao, W. Jiang, L. Du, D. L. Phillips, J. W. Y. Lam, H. H. Y. Sung, I. D. Williams, R. Lu and B. Z. Tang, *J. Am. Chem. Soc.*, 2021, **143**, 9468–9477.
35 Z. G. Chi, X. Q. Zhang, B. J. Xu, X. Zhou, C. P. Ma, Y. Zhang, S. W. Liu and J. R. Xu, *Chem. Soc. Rev.*, 2012, **41**, 3878–3896.
36 J. Zhao, Z. Chi, Y. Zhang, Z. Mao, Z. Yang, E. Ubba and Z. Chi, *J. Mater. Chem. C*, 2018, **6**, 6327–6353.
37 Y. Sagara, S. Yamane, M. Mitani, C. Weder and T. Kato, *Adv. Mater.*, 2016, **28**, 1073–1095.
38 X. Huang, L. Qian, Y. Zhou, M. Liu, Y. Cheng and H. Wu, *J. Mater. Chem. C*, 2018, **6**, 5075–5096.

 This journal is © The Royal Society of Chemistry 2024

Open Access Article. Published on 04 January 2024. Downloaded on 7/20/2025 3:37:24 PM. This article is licensed under a Creative Commons Attribution-NonCommercial 3.0 Unported Licence.

39 W. Z. Yuan, Y. Q. Tan, Y. Y. Gong, P. Lu, J. W. Lam, X. Y. Shen, C. Feng, H. H. Y. Sung, Y. Lu, I. D. Williams and J. Z. Sun, *Adv. Mater.*, 2013, **25**, 2837–2843.
40 S. P. Anthony, *ChemPlusChem*, 2012, **77**, 518–531.
41 S. Gouthaman, A. Jayaraj, M. Suguna Lakshmi, G. Sivaraman and C. A. P. Swamy, *J. Mater. Chem. B*, 2022, **10**, 2238–2250.
42 A. Afrin and C. A. P. Swamy, *New J. Chem.*, 2023, **47**, 18919–18932.
43 (*a*) Z. Yang, Z. Chi, Z. Mao, Y. Zhang, S. Liu, J. Zhao, M. P. Aldred and Z. Chi, *Mater. Chem. Front.*, 2018, **2**, 861–890; (*b*) J. Zhao, Z. Chi, Z. Yang, Z. Mao, Y. Zhang, E. Ubba and Z. Chi, *Mater. Chem. Front.*, 2018, **2**, 1595–1608.
44 J. Li and A. C. Grimsdale, *Chem. Soc. Rev.*, 2010, **39**, 2399–2410.
45 Z. Xu, D. Wu, C. Fang and Y. Li, *Des. Monomers Polym.*, 2023, **26**, 90–105.
46 S. N. Georgiades and P. G. Nicolaou, *Adv. Heterocycl. Chem.*, 2019, **129**, 1–88.
47 L. S. Tsutsumi, D. Gündisch and D. Sun, *Curr. Top. Med. Chem.*, 2016, **16**, 1290–1313.
48 M. S. Shaikh, R. Karpoormath, N. Thapliyal, R. A. Rane, M. B. Palkar, A. M. Faya, H. M. Patel, W. S. Alwan, K. Jain and G. A. Hampannavar, *Anti-Cancer Agents Med. Chem.*, 2015, **15**, 1049–1065.
49 G. Wang, S. Sun and H. Guo, *Eur. J. Med. Chem.*, 2022, **229**, 113999.
50 B. Wex and B. R. Kaafarani, *J. Mater. Chem. C*, 2017, **5**, 8622–8653.
51 S. Oner and M. R. Bryce, *Mater. Chem. Front.*, 2023, **7**, 4304–4338.
52 L. Gao, T. H. Schloemer, F. Zhang, X. Chen, C. Xiao, K. Zhu and A. Sellinger, *ACS Appl. Energy Mater.*, 2020, **3**, 4492–4498.
53 P. Gratia, A. Magomedov, T. Malinauskas, M. Daskeviciene, A. Abate, S. Ahmad, M. Grätzel, V. Getautis and M. K. Nazeeruddin, *Angew. Chem., Int. Ed.*, 2015, **54**, 11409–11413.
54 N. A. Kukhta, T. Matulaitis, D. Volyniuk, K. Ivaniuk, P. Turyk, P. Stakhira, J. V. Grazulevicius and A. P. Monkman, *J. Phys. Chem. Lett.*, 2017, **8**, 6199–6205.
55 M. Hong, M. K. Ravva, P. Winget and J.-L. Brédas, *Chem. Mater.*, 2016, **28**, 5791–5798.
56 P. I. Shih, C. L. Chiang, A. K. Dixit, C. K. Chen, M. C. Yuan, R. Y. Lee, C. T. Chen, E. W. G. Diau and C. F. Shu, *Org. Lett.*, 2006, **8**, 2799–2802.
57 P. Ledwon, *Org. Electron.*, 2019, **75**, 105422.
58 Y. M. Chen, W. Y. Hung, H. W. You, A. Chaskar, H. C. Ting, H. F. Chen, K. T. Wong and Y. H. Liu, *J. Mater. Chem.*, 2011, **21**, 14971–14978.
59 P. R. Hegden, B. D. Emmanuel, J. Beevi and S. S. Dharan, *J. Pharm. Sci. Res.*, 2020, **12**, 1271–1277.
60 N. S. Kumar, P. K. Mukherjee, S. Bhadra, B. P. Saha and B. C. Pal, *Phytother. Res.*, 2010, **24**, 629–631.
61 S. Issa, A. Prandina, N. Bedel, P. Rongved, S. Yous, M. Le Borgne and Z. Bouaziz, *J. Enzyme Inhib. Med. Chem.*, 2019, **34**, 1321–1346.
62 L. Zhu and Y. Zhao, *J. Mater. Chem. C*, 2013, **1**, 1059–1065.
63 A. Gao, Q. Wang, H. Wu, J.-W. Zhao and X. Cao, *Coord. Chem. Rev.*, 2022, **471**, 214753.
64 B. K. An, J. Gierschner and S. Y. Park, *Acc. Chem. Res.*, 2012, **45**, 544–554.
65 B. Kumari, M. Paramasivam, A. Dutta and S. Kanvah, *ACS Omega*, 2018, **3**(12), 17376–17385.
66 S. Sasaki, G. P. C. Drummen and G. Konishi, *J. Mater. Chem. C*, 2016, **4**, 2731–2743.
67 H.-J. Kim, J. Gierschner and S. Y. Park, *J. Mater. Chem. C*, 2020, **8**, 7417–7421.
68 M. Martínez-Abadía, R. Giménez and M. B. Ros, *Adv. Mater.*, 2018, **30**, 1704161.
69 M. Martínez-Abadía, B. Robles-Hernández, B. Villacampa, M. R. de la Fuente, R. Giménez and M. B. Ros, *J. Mater. Chem. C*, 2015, **3**, 3038–3048.
70 K. A. Upamali, L. A. Estrada, P. K. De, X. Cai, J. A. Krause and D. C. Neckers, *Langmuir*, 2011, **27**, 1573–1580.
71 H. Nakano and S. Ōmura, *J. Antibiot.*, 2009, **62**, 17–26.
72 D. Zhang, X. Song, M. Cai, H. Kaji and L. Duan, *Adv. Mater.*, 2018, **30**, 1705406.
73 D. Karthik, S. Y. Lee, D. H. Ahn, H. Lee, J. Y. Lee, J. H. Kwon and J. H. Park, *Org. Electron.*, 2019, **74**, 282–289.
74 W. B. Jia, H. W. Wang, L. M. Yang, H. B. Lu, L. Kong, Y. P. Tian, X.-T. Tao and J. X. Yang, *J. Mater. Chem. C*, 2013, **1**, 7092–7101.
75 Y. Zhang, T. Zhang, X. Wang, L. Kong and J. Yang, *Dyes Pigm.*, 2021, **188**, 109230.
76 Y. Zhang, F. Chen, J. Zheng, Z. Song, Y. Wang, Y. Mao, J. Tang, J. Guo and X. Wang, *CrystEngComm*, 2022, **24**, 7405–7411.
77 Y. Wang, D. Xu, H. Gao, Y. Wang, X. Liu, A. Han, C. Zhang and L. Zang, *Dyes Pigm.*, 2018, **156**, 291–298.
78 Y. Wang, D. Cheng, H. Zhou, J. Liu, X. Liu, J. Cao, A. Han and C. Zhang, *Dyes Pigm.*, 2019, **171**, 107739.
79 Y. Wang, D. Cheng, H. Zhou, X. Liu, Y. Wang, A. Han and C. Zhang, *Dyes Pigm.*, 2019, **171**, 107689.
80 D. Xu, J. Hao, H. Gao, Y. Wang, Y. Wang, X. Liu, A. Han and C. Zhang, *Dyes Pigm.*, 2018, **150**, 293–300.
81 Y. Wang, D. Xu, H. Gao, Y. Wang, X. Liu, A. Han, C. Zhang and L. Zang, *J. Phys. Chem. C*, 2018, **122**, 2297–2306.
82 D. Xu, D. Cheng, Y. Wang, H. Zhou, X. Liu, A. Han and C. Zhang, *Dyes Pigm.*, 2020, **172**, 107786.
83 H. Zhao, Y. Wang, S. Harrington, L. Ma, S. Hu, X. Wu, H. Tang, M. Xue and Y. Wang, *RSC Adv.*, 2016, **6**, 66477–66483.
84 K. Li, Q. Chen and P. Xue, *Tetrahedron*, 2022, **121**, 132924.
85 S. K. Suresh, L. M. Ramachandran, A. Krishnan and C. V. Suneesh, *J. Photochem. Photobiol., A*, 2023, 114985.
86 Q. Zhao, J. He, W. Yang, H. Zhang, L. Lin, F. Jin and Y. Zhan, *Tetrahedron*, 2020, **76**, 131675.
87 M. Tonga, *Tetrahedron Lett.*, 2021, **69**, 152972.
88 J. Xue, F. Tang, A. Ding, F. He, J. Huang, L. Kong and J. Yang, *J. Lumin.*, 2022, **250**, 119119.
89 V. Palakollu and S. Kanvah, *New J. Chem.*, 2014, **38**, 5736–5746.

Open Access Article. Published on 04 January 2024. Downloaded on 7/20/2025 3:37:24 PM.
This article is licensed under a Creative Commons Attribution-NonCommercial 3.0 Unported Licence.

90 P. Jana, M. Paramasivam, S. Khandelwal, A. Dutta and S. Kanvah, *New J. Chem.*, 2020, **44**, 218–230.
91 R. Zuo, S. Wang, Y. Pang, Y. Xiao and Z. Jiang, *Dyes Pigm.*, 2021, **188**, 109153.
92 S. Pei, X. Chen, Z. Zhou, H. Zou and Y. Gong, *Dyes Pigm.*, 2018, **154**, 113–120.
93 J. Xue, F. Tang, C. Wang, J. Yang and A. Ding, *ChemPhotoChem*, 2022, **6**, e202200184.


This journal is © The Royal Society of Chemistry 2024